Journal of Environmental Management 234 (2019) 104–114

Contents lists available at ScienceDirect

Journal of Environmental Management

journal homepage: www.elsevier.com/locate/jenvman

Research article

Quantifying pollutant loading from channel sources: Watershed-scale application of the River Erosion Model

Roderick W. Lammers[a,b,*], Brian P. Bledsoe[b]

[a] Department of Civil & Environmental Engineering, Campus Delivery 1372, Colorado State University, Fort Collins, CO 80523, USA
[b] College of Engineering, Athens, Georgia, USA

ARTICLE INFO

Keywords:
Phosphorus pollution
Sediment pollution
Model uncertainty
Water quality management
Stream restoration

ABSTRACT

Phosphorus and fine sediment pollution are primary causes of water quality degradation. Streambank erosion is a potentially significant source of fine sediment and particulate phosphorus to watersheds, but it remains difficult to quantify the magnitude of this loading. A new, easily applied, watershed scale model was used to simulate the potential for future phosphorus and sediment loading from channel erosion in two watersheds: Big Dry Creek, Colorado and Lick Creek, North Carolina. The projected magnitude of loading for phosphorus is about an order of magnitude higher in Big Dry Creek compared to Lick Creek (~280 kg/yr and ~50 kg/yr, respectively), while sediment loading results are similar (~950 ton/yr). In both watersheds, model results suggest that channel erosion will not contribute a significant amount of phosphorus to the watershed (~1–4% of historic watershed total from all pollutant sources) but will contribute a large amount of sediment (30–100% of historic watershed total). Uncertainty in these estimates is high, but quantifying confidence in model projections is important for understanding and using model results. Importantly, modeling shows no decrease in loading over the 40-year model time frame in either watershed, suggesting that the channels are not adjusting to a new stable state and erosion will continue to be a pollutant source. Lick Creek model results are sensitive to upstream sediment supply while Big Dry Creek's are not, reinforcing the importance of considering alterations to both the hydrologic and sediment regimes when analyzing potential channel changes — at least in vertically active channels. This new modeling approach is useful for estimating historic and future phosphorus and sediment loading from channel erosion, an important first step in effective management to improve water quality.

1. Introduction

Phosphorus and fine sediment are two of the leading causes of water pollution in the United States (U.S. EPA, 2015) and around the world. River channel erosion can be a significant — but highly variable — source of both of these pollutants (Fox et al., 2016). For example, bank erosion can contribute from around 10% (Collins and Walling, 2007) to greater than 90% (Kronvang et al., 1997) of the watershed suspended sediment load. Even within individual watersheds, there is significant inter-annual variability (Palmer et al., 2014) and uncertainty (Thoma et al., 2005). Phosphorus loading from bank erosion is generally lower than that for suspended sediment (both in absolute terms and as a fraction of the total watershed load) but can still be significant (Howe et al., 2011; Kronvang et al., 1997; Ishee et al., 2015). Like fine sediment, phosphorus loading from bank erosion is subject to significant uncertainty depending on the methods used to quantify both erosion and bank phosphorus concentrations (Miller et al., 2014; Purvis et al., 2016).

There are a number of ways to measure bank erosion, depending on the scale and resolution of interest. Bank pins or repeat surveys can be used to measure local erosion rates over months to years (e.g. Beck et al., 2018). Aerial or satellite imagery allows rapid quantification of bank retreat over years to decades at large spatial scales (e.g. Miller et al., 2014; Purvis and Fox, 2016). Repeated Light Detection and Ranging (LiDAR) surveys can provide high spatial resolution data on bank erosion (Thoma et al., 2005), although they can be expensive to collect.

These direct measurement approaches are useful, but they can only be used to estimate historic and current erosion rates. Alternatively, numerical modeling can be used to forecast channel erosion and associated pollutant loading. Modeling has been used to estimate watershed scale sediment and phosphorus loading (Stryker et al., 2017; Langendoen et al., 2012; Mittelstet et al., 2016), and test the effectiveness of channel stabilization measures (Langendoen, 2011; Enlow

* Corresponding author. Boyd Graduate Studies Building, 200 D.W. Brooks Drive, Room 711, Athens, Georgia, 30602, USA.
E-mail address: rodlammers@gmail.com (R.W. Lammers).

https://doi.org/10.1016/j.jenvman.2018.12.074
Received 3 July 2018; Received in revised form 18 December 2018; Accepted 20 December 2018

et al., 2018). The most commonly used model is the Bank Stability and Toe Erosion Model (BSTEM) (Simon et al., 2000, 2011) which has subsequently been integrated into other, more comprehensive models (e.g. Conservational Channel Evolution and Pollutant Transport System (CONCEPTS) (Langendoen and Simon, 2008), Hydraulic Engineering Center - River Analysis System (HEC-RAS) (Gibson et al., 2015), and others (Klavon et al., 2017)). BSTEM has been used for a variety of purposes (Klavon et al., 2017), although most have examined specific erosion mechanisms (Midgley et al., 2012) or the effect of different stabilization or restoration strategies (Langendoen et al., 2012).

Langendoen et al. (2012) used BSTEM to estimate watershed scale sediment and phosphorus loading in the Missisquoi River, Vermont, and to test the effects of different bank grading and riparian planting strategies. Stryker et al. (2017) coupled BSTEM to a hydrologic model to account for the combined effects of upland and in-channel processes on sediment export. These are useful approaches, but do not account for coupled bed and bank erosion. Other models (CONCEPTS and HEC-RAS + BSTEM) do account for these two modes of channel adjustment, but may be better suited for reach scale application because they can be difficult to parameterize and apply at the watershed scale.

The objective of this paper is to expand on these past modeling efforts by using a new physically based yet parsimonious model to simulate future sediment and phosphorus loading from channel erosion. The River Erosion Model (REM) (Lammers and Bledsoe, 2018a; Lammers, 2018) simulates both bed and bank erosion at the watershed scale — accounting for how channel evolution in one part of the watershed can influence sediment dynamics in other reaches. Channels responding to disturbance evolve in complex ways (Schumm et al., 1984; Simon, 1989; Booth and Fischenich, 2015; Cluer and Thorne, 2014) and accounting for the dominant mechanisms of channel evolution is essential for accurately quantifying water quality impacts. Understanding the magnitude of pollutant loading from channel erosion relative to other sources (e.g. wastewater treatment facilities, urban stormwater runoff, and agriculture), is essential for successful and cost-effective water quality management. Importantly, REM is built to run Monte Carlo simulations — allowing users to quantify uncertainty in model projections.

2. Study watersheds

REM was applied to two watersheds: Big Dry Creek in Colorado and Lick Creek in North Carolina. These two examples represent very different climates (semi-arid vs. humid) and history (past vs. recent urbanization), providing illustrative examples of the how REM can be used in diverse landscapes.

2.1. Big Dry Creek, Colorado

Big Dry Creek is a 280 km^2 watershed located in the northern suburbs of Denver on the Front Range of Colorado. The bed material is primarily sand, but with some gravel in the upper reaches. Streambank material is mostly clay and sandy clay loam. Riparian areas consist of grasses, willows, Russian olive, and some cottonwoods. The upper portion of the watershed is mostly undeveloped, but with a growing urban area in the middle. Most of the lower third of the watershed is agricultural land (Fig. 1). A management goal has been set to reduce phosphorus loading from Big Dry Creek as part of a total maximum daily load (TMDL) plan for the Barr-Milton watershed (Clary, 2017). In addition, total phosphorus concentrations in much of Big Dry Creek regularly exceed forthcoming in-stream nutrient standards set by the State of Colorado (Clary, 2017).

The hydrologic regime of Big Dry Creek has been significantly altered. Standley Lake, a reservoir in the upstream part of the basin, was constructed in 1912 to provide irrigation water to downstream farms. Today, the reservoir also serves as a municipal drinking water source but releases are still highly managed to supply water to downstream users. The watershed has also seen two population booms — one in the 1970s and the other starting in the 1990s and continuing until today. This rapid development has increased stormwater runoff to the stream. Furthermore, three wastewater treatment plants in the watershed provide a near continuous baseflow to Big Dry Creek. These hydrologic alterations — irrigation releases, increased stormwater runoff, and wastewater treatment effluent – have led to significant channel degradation.

2.2. Lick Creek, North Carolina

Lick Creek is a 38 km^2 watershed located on the outskirts of Durham, NC. Land cover is primarily forest with small portions of agricultural land and expanding development in the headwaters. Development and agriculture are mostly limited to the uplands while the valley floor is extensively forested (Fig. 2). The bed material is primarily sand but with some clay and isolated bedrock outcrops. Streambank material is mostly loam, clay loam, and sandy loam. There are also a number of relict and active beaver dams on the tributaries. The lower main stem of Lick Creek has incised and widened. This incision is migrating upstream into the tributaries and two active knickpoints were identified during field data collection. Lick Creek is currently listed as impaired for aquatic life. The creek drains to Falls Lake reservoir, which is subject to a nutrient reduction plan and is currently listed as impaired due to high turbidity (North Carolina Department of Environmental Quality, 2016).

3. Methods

3.1. The River Erosion Model

REM simulates channel evolution based on specific stream power (a function of channel slope, width, and discharge) eliminating the need for detailed hydraulic calculations of flow depth and shear stress. Changes in channel bed elevation are computed based on a sediment mass balance: erosion occurs if sediment transport capacity exceeds supply while deposition occurs when supply exceeds capacity. Sediment transport by grain size is modeled using new stream power based bedload and total load transport equations (Lammers and Bledsoe, 2018b):

$$q_b = 1.43 \times 10^{-4}(\omega - \omega_c)^{3/2} D_s^{-1/2} q^{-1/2} \quad (1)$$

$$Q_t = 0.0214(\omega - \omega_c)^{3/2} D_s^{-1} q^{-5/6} \quad (2)$$

where q_b is the mass bedload sediment transport rate per unit width [kg m^{-1} s^{-1}], Q_t is the total load [ppm], q is unit discharge [m^2 s^{-1}], D_s is the grain size [m], ω is specific stream power [W m^{-2}], and ω_c is the critical specific stream power for incipient motion [W m^{-2}]. Channel incision into cohesive material can also be simulated using an excess shear stress approach (Partheniades, 1965):

$$E = k\Delta t(\tau - \tau_c) \quad (3)$$

where E is the erosion distance [m], k is the erodibility coefficient [m^3 N^{-1} s^{-1}], Δt is the time step [s], τ_c is the critical shear stress of the bed material [Pa], and τ is the applied shear stress [Pa] which is calculated directly from specific stream power using a new empirical relationship (Lammers and Bledsoe, 2018a):

$$\tau = 1.96\omega^{0.72} \quad (4)$$

REM simulates both fluvial bank erosion and bank failure using a modified version of the Bank Stability and Toe Erosion Model (BSTEM) (Simon et al., 2000, 2011). This requires two primary bank soil parameters: bank critical shear stress and bank soil cohesion. Channel bed elevation and width are updated as the bed incises/aggrades and the banks erode. Finally, the model can also account for knickpoint migration (Allen et al., 2018), leading to abrupt channel deepening as the

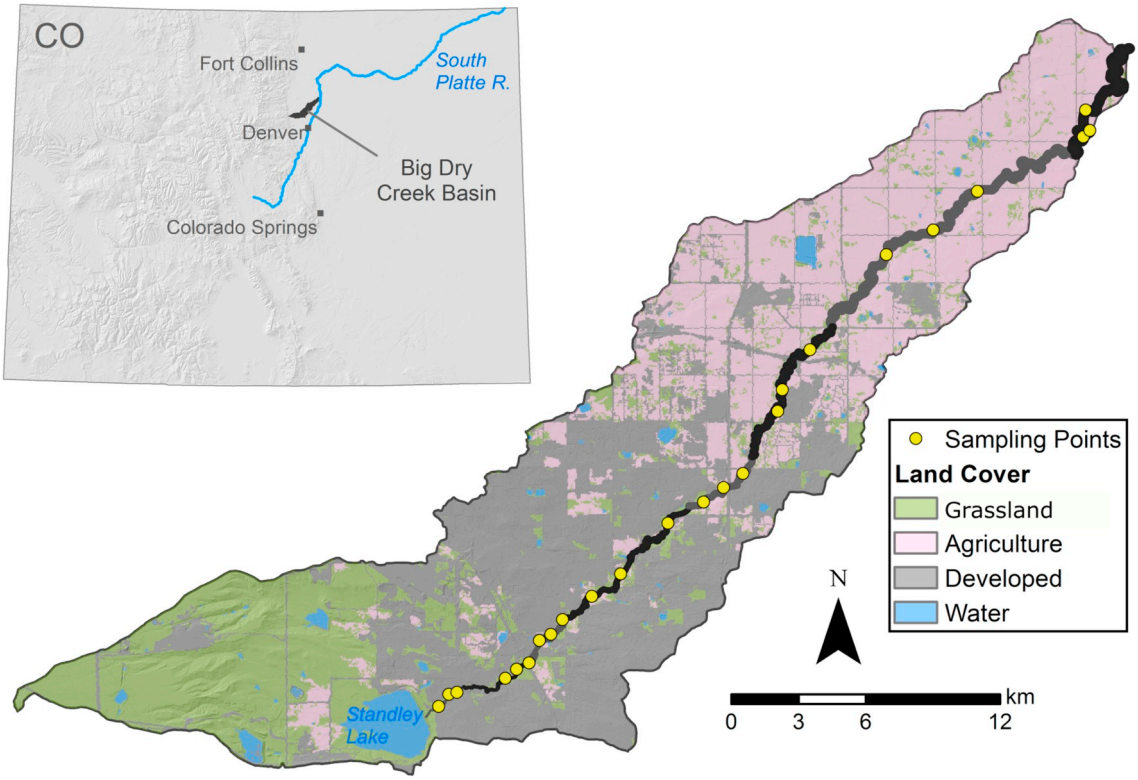

Fig. 1. Big Dry Creek watershed. Land use is 24% undeveloped grassland, 33% agriculture, 40% developed, and 3% water (National Land Cover Database (NLCD) 2011; Homer et al. (2015)).

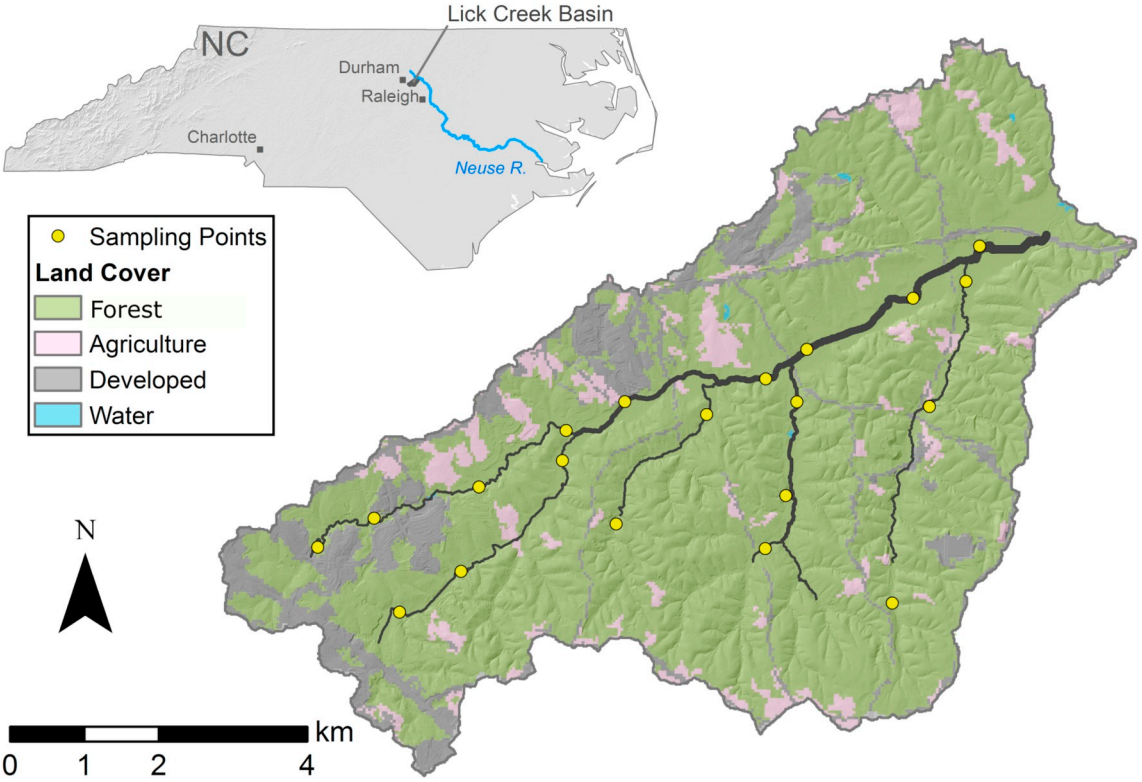

Fig. 2. Lick Creek watershed. Land use is 80% undeveloped forest, 7% agriculture, and 13% developed (NLCD 2011; Homer et al. (2015)).

knickpoint migrates past a cross section, and channel meandering, which increases channel sinuosity and reduces slope. A user-specified fraction of eroded bank, knickpoint, and cohesive bed material is added to the bed material load (sand and coarser). The remainder is assumed to be washload (silt and clay) that is all transported to the watershed outlet (i.e. no in-channel or floodplain storage). All model estimates of

sediment and phosphorus loading are from this washload material. For a more detailed description of REM see Lammers (2018) and Lammers and Bledsoe (2018a).

3.2. Data collection and model application

During summer 2015, field data were collected at 24 sites along Big Dry Creek (Fig. 1). Prior to the field campaign, the channel was divided into eight reaches that had relatively homogeneous land use and riparian conditions. Where possible, reaches were separated at major grade controls (e.g. road crossings, diversion structures, or bed stabilization structures). Bank geometries were measured at three sites within each of the eight reaches. Three soil samples per site (from the top, middle, and toe of one bank) were collected and analyzed for phosphorus content and soil texture. Soil samples were processed by the Soil, Water, and Plant Testing Laboratory at Colorado State University for total phosphorus (TP; EPA Method 3050a), Mehlich-3 P, and water extractable P. Channel longitudinal profiles and channel widths were obtained from a LiDAR-derived Digital Elevation Model (DEM) (0.75 m resolution) from October 2013 (geodata.co.gov). To estimate historic erosion rates, channel banks were delineated from 1993 to 2014 aerial imagery (Google Earth Pro, 2017). The two channel polygons were overlayed and the eroded areas were calculated based on differences in channel position. Based on repeat delineation of the same 3 km reach, average errors were 1.4–1.8 m. Therefore, only erosion estimates that were greater than 2 m were used to incorporate these errors and unknown orthorectification errors. Bank heights, soil bulk densities, and phosphorus concentrations were then used to estimate sediment and phosphorus loading over this time period. Changes in channel width and sinuosity between 1993 and 2014 were also quantified and the significance of changes was assessed using the Wilcoxon Signed Rank Test.

In spring 2016 field data were collected at 20 sites along Lick Creek and its major tributaries (Fig. 2), following the same data collection procedure as for Big Dry Creek. Channel longitudinal profiles, channel widths, and floodplain widths and slopes were obtained from a 1 m resolution DEM constructed from LiDAR data collected in early 2015 (sdd.nc.gov/sdd). The stream network was delineated and channel geometry data were extracted for both watersheds using the hydro-geomorphological Geographic Information System (GIS) tool developed by Biron et al. (2013). Historic erosion rates for Lick Creek could not be determined using aerial imagery because the narrow stream and dense canopy made it impossible to see the channel banks.

3.2.1. Estimating bank cohesion

Logistic regression analysis of bank heights and angles was used to estimate soil cohesion (Bledsoe et al., 2012). Logistic regression predicts the probability of bank failure (p) based on bank angle (α) and height (H):

$$\ln \frac{p}{1-p} = \beta_o + \beta_\alpha \ln \alpha + \beta_H \ln H \tag{5}$$

where β_o, β_α, and β_H are fitted model coefficients.

This model was fit to field data on bank heights and angles for stable ($p = 0$) and unstable ($p = 1$) banks. The logistic regression model solved for $p = 0.5$ (assumed equal to the critical bank height for failure) was used in conjunction with the Culmann equation for geotechnical slab failure to estimate the effective cohesion of the bank material (c', kPa):

$$c' = \frac{\gamma(1 - \cos(\alpha - \phi'))\exp\left(\frac{-\beta_o}{\beta_H} - \frac{\beta_\alpha}{\beta_H}\ln \alpha\right)}{4 \sin \alpha \cos \phi'} \tag{6}$$

where γ is the unit weight of the soil [kN m^{-3}] and ϕ' is the effective friction angle of the bank material [degrees]. ϕ' was assumed to vary uniformly between 11. 4° and 32. 3°, γ between 16.9 and 19.2 kN m^{-3} (Simon et al., 2011), and α between 40° and 90°. This yielded a mean c' value of 1.4 kPa (standard deviation = 0.4) for Big Dry Creek and 2.1 kPa (standard deviation = 2.0) for Lick Creek (see the Supplementary Material for fitted logistic regression models). These cohesion estimates account for a variety of sources of bank strength (including vegetation) and may be considered operational shear strengths (Bledsoe et al., 2012).

3.2.2. Estimating bank critical shear stress

Critical shear stress (τ_c) of bank material in both watersheds was estimated using measured erosion rates and U.S. Geological Survey (USGS) gage data. For Lick Creek, erosion data collected by the City of Durham from nearby Ellerbe Creek, located near USGS gage 0208675010 was used. Lick and Ellerbe creeks both have Triassic soils (Voli et al., 2013), so it was assumed their bank soils have similar erosion resistance. Specific stream power was calculated using 15 min flow data and DEM-derived channel slope and width. These stream power values were converted to a wall shear stress using the same empirical equation used by REM. The value of τ_c that best approximated observed erosion rates was then calculated (Supplementary Material). A similar approach was used for Big Dry Creek, using 15 min and hourly flow data from USGS gage 06720820 and bank erosion rates estimated from the aerial imagery analysis. Soil erodibility was calculated by REM from given τ_c values using the empirical relationship developed by Simon et al. (2010).

3.2.3. Hydrology

For Big Dry Creek, daily flow data from two USGS gages were used, one in the urbanized area of the watershed (06720820) and the other at the watershed outlet (06720990). Peak flows and flashiness have both increased in the watershed over the period of record. Therefore, flow data from Jan. 2006–Dec. 2017 was used as representative of the future hydrology of the basin. Discharge for each modeled reach was calculated based on drainage area, while accounting for releases from Standley Lake (summer only) and two wastewater treatment plants (year round) as well as withdrawals from five irrigation ditches (summer only). A 41 year flow record (2013–2053) was constructed with flow data from 2013 to 2017 (corresponding to initial DEM-derived channel geometry from 2013) plus repeating the 12 years of historic flow data (2006–2017) three times. A simulation was also run over the same time period using 15 min flow data. Results were nearly unchanged but computation time increased significantly; therefore, only daily flow data was used.

For Lick Creek, there are no current or historic flow data. Instead, daily flow data from Little Lick Creek (USGS 0208700780) was used, which is the watershed directly adjacent. These daily data were available for Oct. 1982–Sep. 1995. These flow data were expected to be representative of current and future conditions in Lick Creek because the watershed population density is currently increasing at a similar rate as Little Lick Creek did from 1982 to 1995 (Supplementary Material). Flows in each modeled reach were scaled based on drainage area. These 13 years of data were repeated three times to give a total model simulation of 39 years (2015 (year of DEM) through 2053).

3.2.4. Model application

REM was applied to Big Dry Creek using a cross section spacing of 500 m and a time step of 900 s. Two simulations were run with different upstream sediment supply: Q_s = 0.5 and 1.0 of transport capacity. The total load sediment transport equation was used to model grain sizes smaller than 4 mm, and the bedload equation for all coarser material. Five grade control structures were included (i.e. putting a non-erodible cohesive bed at these locations) (Table S1). Eight reaches with unique channel geometries (but the same bank soil properties) were modeled. Modeled annual sediment and phosphorus loads from channel erosion were compared to historic total annual loads calculated from monthly in-stream water quality data (courtesy of the Big Dry Creek Watershed

Association) and flow data from the USGS gage at the watershed outlet.

For Lick Creek, a cross section spacing of 200 m, time step of 2400 s, and uniform grain size of 2 mm (total load transport equation) were used. Four grade controls (roads and bedrock outcrops) were incorporated. For the remaining cross sections, a clay layer was assumed to be 2 m below the alluvium with the same τ_c as the bank material. This was based on field observations of exposed clay bed material in incising channels. Two knickpoints were observed during the field campaign. Knickpoint erodibility coefficients were calibrated to match observed migration rates from 2001 to 2015 (see the Supplementary Material). Since there is no information on upstream sediment supply, three simulations were run with different rates: Q_s = 0.5, 0.75, and 1.0 of transport capacity (Table S2). Eleven reaches with unique channel geometries (but the same bank soil properties) were modeled. Measured monthly sediment and phosphorus water quality data for Lick Creek were obtained from the City of Durham and Upper Neuse River Basin Association. Since there is no gage on this stream, annual loads could not be calculated. Instead, modeled loads were converted to concentrations (annual load/annual flow volume) to compare to these measured data. For both watersheds, measured bank total phosphorus concentrations were used, as described above. For both watersheds, 1000 Monte Carlo simulations were run varying model inputs (Tables S1 and S2) to quantify preliminary uncertainty in model projections. The Mann-Kendall trend test was used to determine if there were any trends in modeled pollutant loading through time. All data analyses were performed in R version 3.4.4 (R Core Team, 2018).

3.3. Sensitivity analyses

Sensitivity analyses of each model output were performed using the Plischke et al. (2013) density-based method. These analyses quantify the impact of each input variable on uncertainty in model output from the Monte Carlo simulations. For each simulation, uncertainty was quantified for predicted phosphorus loading, sediment loading, bed elevation, and channel width. To give a single output value for bed elevation and channel width, the absolute value of total change in the variable across all cross sections was summed. For the loading variables, the median annual load from each Monte Carlo simulation was used.

4. Results

4.1. Historic and current erosion

4.1.1. Big Dry Creek

Incision is widespread in Big Dry Creek, as evidenced by the tall steep banks throughout much of the watershed (median height = 1.4 m, max = 5 m; median angle = 60°, max = 90°). Given the little visible evidence of recent bed erosion, however, it appears this incision has slowed or halted because of artificial (e.g. rock structures) and natural (e.g. clay soil) grade controls. As the channel is now mostly vertically stable, it has recently adjusted primarily via bank erosion and lateral channel migration. The aerial imagery analysis provided additional evidence of this (Fig. 3). There was a mix of widening and narrowing along the channel from 1993 to 2014, but the average change in channel width was not significant. Sinuosity, on the other hand, did show a slight but statistically significant increase over this period (median increase of 0.04; $p < 0.0001$; Wilcoxon Signed Rank Test). Much of the upper portion of the watershed was observed to be in the later stages of channel evolution (stages IV–V in the Schumm et al. (1984) channel evolution model, CEM). The channels in the lower half of the watershed have not widened as significantly, and are currently in stage II (incision or arrested incision) or III (widening) of the CEM (Fig. S4). Big Dry Creek is still evolving and it is unclear when it will restabilize.

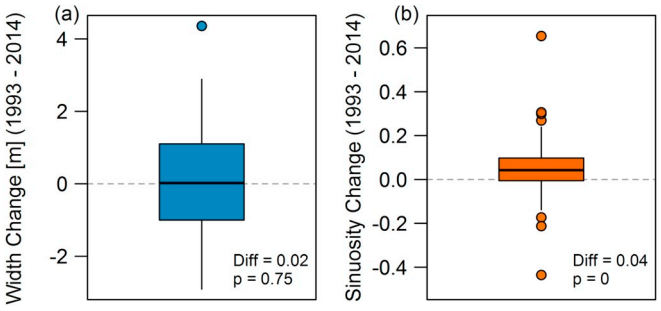

Fig. 3. Changes in channel width (a) and sinuosity (b) in Big Dry Creek from 1993 to 2014 for the same, 1 km long reaches. Values estimated using digitized stream channels from aerial imagery. Boxplots show median (middle bar), quartiles (box), non-outlier maximum and minimum (1.5 times the interquartile range), and outliers (points). The median difference and p-value of a Wilcoxon Signed Rank Test are shown. These tests suggest the width change was not significantly different from zero but that sinuosity showed a statistically significant increase over the observation period.

4.1.2. Lick Creek

The channels in Lick Creek are actively evolving, presumably in response to changes in runoff and sediment supply caused by ongoing development. Much of the main stem has incised and widened, and this incision is currently migrating up the tributaries (Fig. S5). There is significant sand deposition in the lower reaches of Lick Creek, probably as a result of high sand loading from upstream bed and bank erosion. These lower aggrading reaches are in stage IV of the CEM (aggrading and widening), while the tributaries are all in stages II–III (incising and widening). Development will likely continue into the future, further destabilizing the stream. There are several bedrock outcrops serving as local grade controls but these may not be sufficient to keep the channels from significantly incising and widening in response to this watershed disturbance.

4.2. Bank phosphorus concentrations

Fig. 4 shows bank total phosphorus concentrations from Big Dry Creek and Lick Creek compared to data from 15 other studies (Lammers and Bledsoe, 2017). Big Dry Creek's bank phosphorus content is similar to these other data, but Lick Creek has extremely low values (with the exception of one outlier > 1800 mg/kg). For both watersheds,

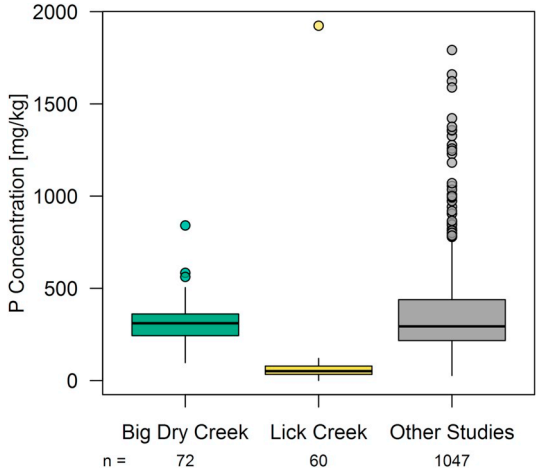

Fig. 4. Measured bank total phosphorus concentrations for the two study watersheds compared to data from 15 other studies (Lammers and Bledsoe, 2017). Boxplots show median (middle bar), quartiles (box), non-outlier maximum and minimum (1.5 times the interquartile range), and outliers (points). Bank soil samples collected August 2015 (Big Dry Creek) and March 2016 (Lick Creek).

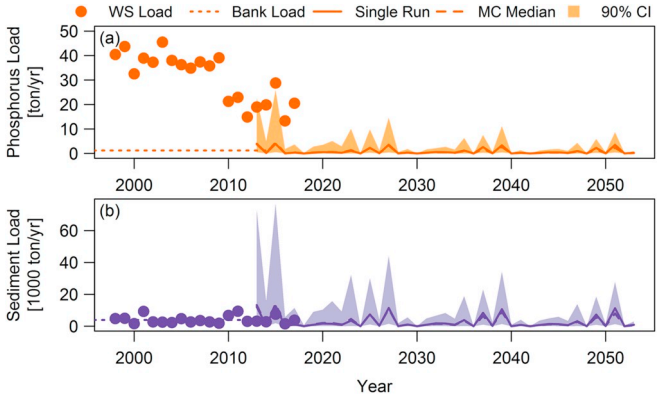

Fig. 5. Observed (points) and modeled (lines) annual loads of phosphorus (a) and sediment (b) for Big Dry Creek. Historic measured watershed loads are shown as points, bank loading estimates from the aerial photo analysis (1993–2014) are shown as a horizontal dotted line, and model results for future loading for the single model run (solid line), median of the Monte Carlo simulations (dashed line), and 90% CI are projected through 2053. Model results are from simulations with Q_s = 0.5. Ton = 1000 kg.

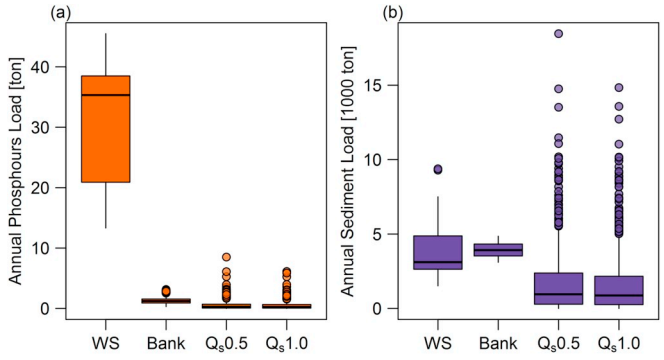

Fig. 6. Distributions of predicted median annual phosphorus (a) and sediment (b) loads for the two modeled scenarios from Big Dry Creek: Q_s = 0.5 and Q_s = 1.0 (2013–2053). These are compared to estimates of annual loading from bank erosion from the aerial imagery analysis (1993–2014; Bank) and measured watershed loads from 1998 to 2017 (WS). Boxplots show median (middle bar), quartiles (box), non-outlier maximum and minimum (1.5 times the interquartile range), and outliers (points). Ton = 1000 kg.

concentrations of Mehlich-3 phosphorus and water extractable phosphorus are about 10% and 5% of total phosphorus concentrations, respectively. These extraction methods may be more representative of bioavailable phosphorus than the TP concentrations shown here; however, total phosphorus loading was modeled to compare with measured data (using total phosphorus loads and concentrations) and because most regulations focus on total phosphorus.

4.3. Projected phosphorus and sediment loading from channel erosion

4.3.1. Big Dry Creek

Fig. 5 shows modeled annual phosphorus and sediment loads in Big Dry Creek from channel erosion (2013–2053, with uncertainty) from the Q_s = 0.5 simulation, compared to measured annual loads at the watershed outlet (1997–2017). Bank loading estimates from the aerial analysis (1993–2014) are also shown. The results from the single model run and median of the Monte Carlo simulations are essentially identical. There is significant inter-annual variability in the projected loads, and the peaks of the uncertainty range do appear to decrease over time. There is not, however, any statistically significant trend in the median results (Mann-Kendall trend test, p = 0.57 for both Q_s = 0.5 and 1.0 simulations).

Fig. 6 compares distributions of median annual loads from the two model simulations (Q_s = 0.5 and Q_s = 1.0) with the historic observed watershed load and bank loading estimate from the aerial imagery analysis. The two model simulations show nearly identical results. The modeled median annual phosphorus load (median = 0.3 ton/yr; 0.005–1.8 ton/yr 90% confidence interval [CI]) was one quarter of the aerial imagery analysis estimate (1.2 ton/yr). Both are significantly less than the historic measured watershed TP load (median = 35 ton/yr). Modeled median annual sediment loads (median = 950 ton/yr; 17–5600 ton/yr 90% CI) are also less than both the historic watershed load (3100 ton/yr) and aerial imagery estimate (3900 ton/yr). These results indicate that future phosphorus loading from channel erosion could be small relative to the historic watershed load (median ~1%, 0.01–5% 90% CI) but that future sediment loading could be a significant percentage (median = 31%; 0.5–180% 90% CI) of the historic watershed sediment load. Table 1 summarizes modeled median annual loadings of both phosphorus and sediment.

Fig. 7 shows modeled sediment loading rates by reach, with uncertainty (Q_s = 0.5 simulation). Sediment loading was relatively consistent throughout the channel network, although the most upstream reach did have consistently higher rates than others. The spatial distribution of phosphorus loading is identical and is therefore not shown. Plots of pollutant loading, channel incision, channel widening, and sensitivity analysis results for both simulations are included in the Supplementary Material.

Big Dry Creek modeling shows little change in bed elevations throughout the watershed — consistent with field observations that the channel is relatively stable vertically (Figs. S4 and S8). Modeling does, however, predict slight widening (1–2 m; Figs. S7 and S11) and increases in channel sinuosity (median increase ~0.15). The aerial imagery analysis showed no net change in channel width (Fig. 3), although 1–2 m of widening is certainly within the range of observations. This historic analysis also showed a general increase in channel sinuosity, although at smaller annual rates (0.002/year) than what modeling predicts (0.0035/year). Taken together, these results suggest that the channel will continue to adjust via a mix of widening and increased sinuosity, with only localized bed aggradation or incision.

4.3.2. Lick Creek

Fig. 8 shows modeled average annual total phosphorus (TP) and total suspended solids (TSS) concentrations in Lick Creek from channel erosion (2015–2053, Q_s = 0.5 simulation), with uncertainty, compared to historic measured values at the watershed outlet (2004–2017). There is some inter-annual variability in modeled concentrations, especially in the peaks of the 90% CI. There is not, however, an obvious increase or decrease in concentrations with time. A Mann-Kendall trend test confirms there is no statistically significant trend for any simulation (Q_s = 0.5: p = 0.36; Q_s = 0.75: p = 0.96; Q_s = 1.0: p = 0.08).

Fig. 9 compares distributions of modeled median annual TP and TSS concentrations for the three simulations to measured values. Modeled concentrations decrease as upstream sediment supply increases. For all simulations, modeled TSS concentrations are at or above historic observations while TP concentrations are significantly less than measured values. Modeled median annual TP concentrations (median = 0.003 mg/L; 0.0002–0.009 mg/L 90% CI) are an order of magnitude lower than observed values (median = 0.08 mg/L). Modeled median annual TSS (median = 59 mg/L; 31–131 mg/L 90% CI) is higher than observations (median = 29 mg/L). These model results for the Q_s = 0.5 simulation suggest that future channel erosion could contribute > 100% (median = 203%; 106–450% 90% CI) of the historic fine sediment pollution in Lick Creek, but only ~4% (0.3–11% 90% CI) of the historic phosphorus.

Fig. 10 shows modeled sediment loading by reach over the course of the simulation (Q_s = 0.5). Two reaches had consistently higher loading throughout all the Monte Carlo simulations. Both reaches had actively migrating knickpoints which likely contributed to high modeled

Table 1
Modeled median annual total phosphorus and sediment loading from channel erosion in Big Dry Creek and Lick Creek. Median values are shown with 90% CI in parentheses. Ton = 1000 kg.

Simulation	Annual P Load [kg/yr]	Annual P Load [kg/km/yr]	Annual Sed Load [ton/yr]	Annual Sed Load [ton/km/yr]
Big Dry Creek, Q_s = 0.5	285 (5–1800)	4.8 (0.1–31)	950 (17–5600)	16.2 (0.3–95)
Big Dry Creek, Q_s = 1.0	255 (4–1770)	4.3 (0.1–30)	875 (16–5400)	14.8 (0.3–91)
Lick Creek, Q_s = 0.5	48 (4–140)	1.8 (0.1–5.3)	940 (460–2060)	35 (17–77)
Lick Creek, Q_s = 0.75	42 (3–124)	1.6 (0.1–4.7)	820 (410–1850)	31 (15–69)
Lick Creek, Q_s = 1.0	27 (2–73)	1.0 (0.1–2.7)	520 (270–1100)	19 (10–41)

sediment loads. The spatial distribution of phosphorus loading is identical, therefore these data are not shown.

The median of the modeled annual phosphorus load (Q_s = 0.5 simulation) was 48 kg/yr (4–140 kg/yr 90% CI). Median annual sediment loading was 940 ton/yr (460–2060 ton/yr 90% CI). Similar to the concentration data, modeled loads for the low sediment supply simulation were higher than the other two (Table 1). Plots of pollutant loading, channel incision, channel widening, and sensitivity analysis results for all three simulations are included in the Supplementary Material.

Modeled channel changes in Lick Creek are consistent with field observations, with channel incision (and some local aggradation) predicted in the tributaries and aggradation along the mainstem. This indicates that recent observed channel response will continue into the future. The model also predicts channel widening generally throughout the watershed, suggesting that even the aggrading lower reaches are still susceptible to bank erosion. These trends are consistent across both the Q_s = 0.5 and Q_s = 0.75 simulations, while the Q_s = 1.0 run shows much more widespread aggradation due to higher upstream sediment supply (see Supplementary Material). Modeled estimates of loading decreased as sediment supply increased (Fig. S14); although, uncertainty within each simulation is large relative to the differences among simulations.

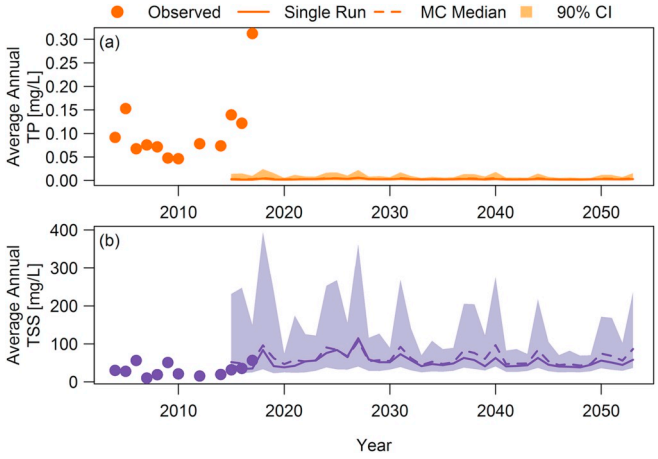

Fig. 8. Observed (points) and modeled (lines) average annual concentrations of TP (a) and TSS (b) for Lick Creek. Historic measured concentrations at the watershed outlet are shown as points. The model results for the single model run (solid line), median of the Monte Carlo simulations (dashed line), and the 90% CI are projected through 2053. Model results from simulations with Q_s = 0.5.

5. Discussion

5.1. Significance of channel erosion as a pollutant source

For both Big Dry Creek and Lick Creek, model simulations suggest channel erosion will be a minor source of phosphorus (~1–4% of historic total watershed load or concentration) but may contribute 30–200% as much fine sediment pollution as has been recently measured from all sources in the watershed. These percentages assume that historic observed loads (Big Dry Creek) and concentrations (Lick Creek) at the watershed outlets are representative of future conditions. The fact that model simulations for Lick Creek are higher than observed TSS concentrations either suggests the model is overpredicting loading from channel erosion, estimates of annual average TSS concentrations based on monthly measurements are inaccurate, or that watershed pollutant loading could increase in the future due to continued channel instability.

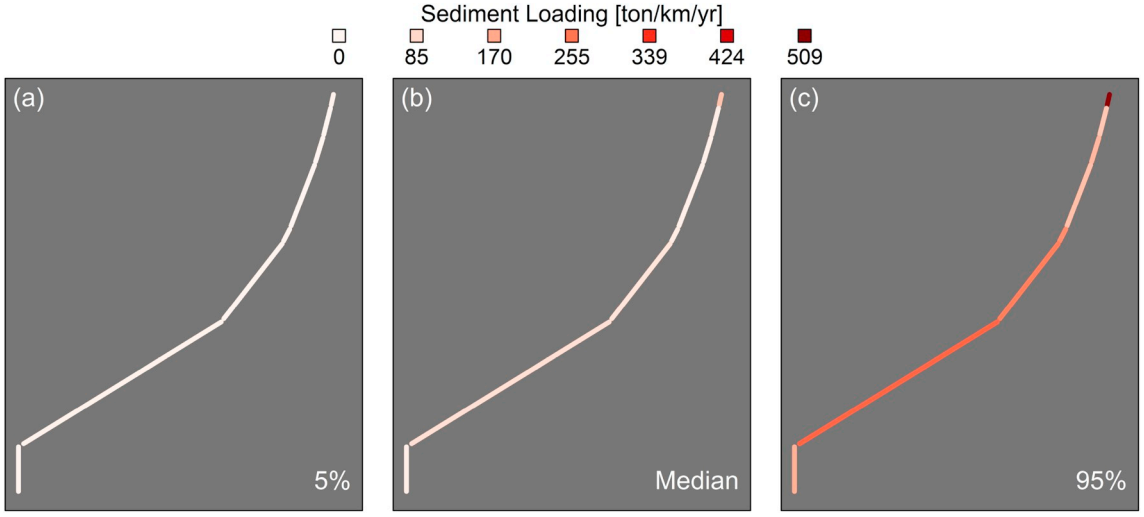

Fig. 7. Network schematic of Big Dry Creek showing annual sediment loading rates by modeled reach, normalized by reach length, including the uncertainty range (a and c) and the median of the Monte Carlo results (b). Loading rates are larger than reported in Table 1 because these are cumulative loads over the simulation rather than median annual loads. Results from simulation with Q_s = 0.5. Ton = 1000 kg.

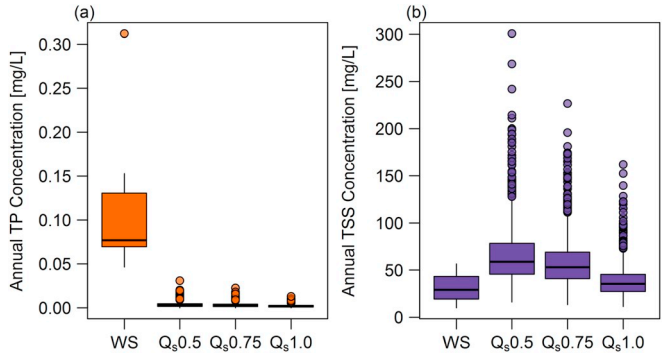

Fig. 9. Distributions of median annual predicted TP (a) and TSS (b) concentrations for Lick Creek across the years of the simulation, for the three different modeled scenarios: Q_s = 0.5, Q_s = 0.75, and Q_s = 1.0 of transport capacity. These are compared to the distributions of observed annual TP and TSS concentrations at the watershed outlet from 2004 to 2017. Boxplots show median (middle bar), quartiles (box), non-outlier maximum and minimum (1.5 times the interquartile range), and outliers (points).

The relative importance of channel erosion for phosphorus and sediment pollution is consistent for both watersheds, but the reasons for this consistency differ. For Big Dry Creek, two large wastewater treatment plants are likely responsible for most of the watershed phosphorus load, while contributing little or no suspended sediment. In fact, the significant drop in the watershed phosphorus load since 2010 (Fig. 5) has been attributed to improved phosphorus removal at these facilities (Clary, 2017). In Lick Creek, on the other hand, modeled phosphorus loading is extremely small because of the naturally low abundance of phosphorus in streambank soils.

Phosphorus and sediment loading rates per unit stream length in Big Dry Creek (Table 1) are on the low end but of similar order of magnitude to eroding streams in Iowa (Zaimes et al., 2008; Tufekcioglu, 2010; Nellesen et al., 2011), Missouri (Peacher, 2011), and Denmark (Kronvang et al., 2012). They are one to two orders of magnitude less than model estimates of loading from Vermont (Langendoen et al., 2012) and Oklahoma (Miller et al., 2014) and from erosion of millpond sediment in Pennsylvania (Walter et al., 2007) (Lammers and Bledsoe, 2017, Table 1). This suggests that modeled loading estimates are similar to what has been observed in other eroding streams of similar size. Lick Creek's normalized sediment loading rates are also similar to these other studies, but predicted phosphorus loading is lower than what has been observed elsewhere. This is expected given the low phosphorus abundance in Lick Creek streambanks.

Low measured bank phosphorus content in Lick Creek is not surprising given that North Carolina — and most of the southeastern coastal plain — has low soil phosphorus abundance (Smith et al., 2013). Bank phosphorus concentrations for both Lick Creek and Big Dry Creek show significant spatial variability, but there are not any observable trends. Other studies have found that bank phosphorus is correlated with location in the watershed (Miller et al., 2014), position on the bank (Bledsoe et al., 2000; Purvis et al., 2016), soil silt-clay content (Cooper and Gilliam, 1987; Bledsoe et al., 2000; Agudelo et al., 2011; Kerr et al., 2011; Young et al., 2012), and land use (Palmer-Felgate et al., 2009; Haggard et al., 2007). None of these variables were correlated with bank total phosphorus in the study watersheds. Still, uncertainty in bank phosphorus content can introduce significant uncertainty into modeled phosphorus loading. This was the case in Lick Creek where loading was predominately from cohesive bed and knickpoint erosion (Figs. S15, S20, and S25). In Big Dry Creek, however, high uncertainty in phosphorus loading was almost exclusively because of bank τ_c — indicating that the magnitude of bank erosion was more important for loading than variability in bank phosphorus content (Figs. S6 and S11).

The temporal overlap between the beginning of the model simulation and observed data is useful for evaluating model accuracy; however, neither model was calibrated to these measured water quality data and the daily flow record used in the Lick Creek models does not necessarily match actual flows over this time period. The point of including this historic data is instead to assess the magnitude of modeled loading versus past observations.

In Big Dry Creek, the first several years of the simulation show sediment loading that is similar to total watershed sediment loads. Similar peaks in annual sediment loading are obvious throughout the remainder of the simulation and show that high discharge years lead to high pollutant loading from channel erosion. Despite these peaks, median annual sediment loading is only about one third of historic total watershed sediment loads. Model predictions for both phosphorus and sediment are less than historic bank erosion loading estimates from the aerial imagery analysis. This could indicate that future pollutant loading from channel erosion will be less than average loading that has been observed over the last two decades.

In Lick Creek, the three years of overlap between the simulations and observed data (2015–2017) show remarkable agreement between measured and modeled TSS concentrations. Throughout the remainder of the

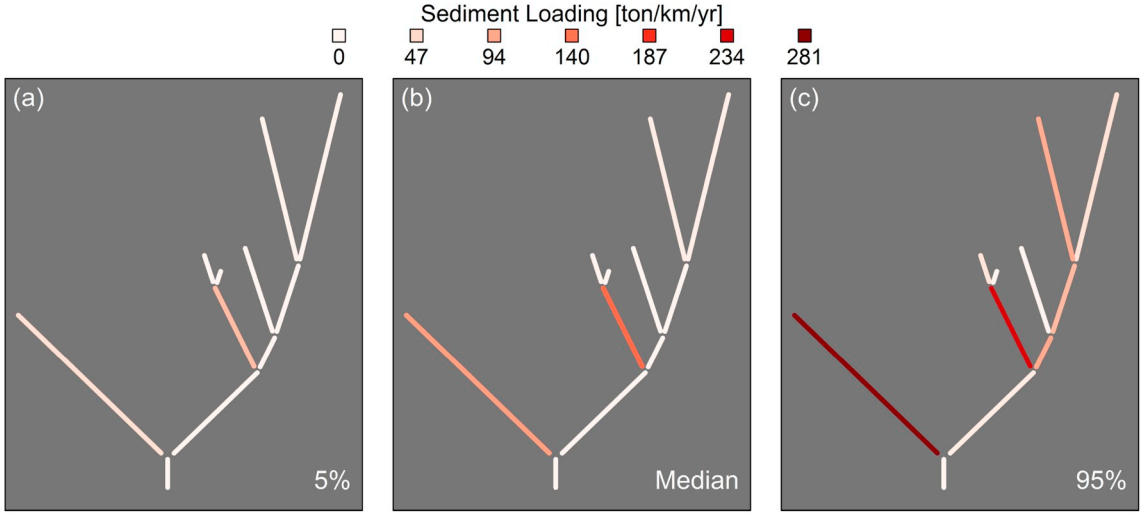

Fig. 10. Network schematic of Lick Creek showing annual sediment loading rates by modeled reach, normalized by reach length including the uncertainty range (a and c) and the median of the Monte Carlo results (b). The two reaches with highest loading rates both had actively migrating knickpoints. Loading rates are larger than reported in Table 1 because these are cumulative loads over the simulation rather than median annual loads. Results from simulation with Q_s = 0.5.

simulation, modeled TSS remains high. Model results, however, do not take into account other sources of fine sediment pollution. Sediment fingerprinting from 2011 showed that bank erosion contributed only 25% (11–43% ± one standard deviation) of the total suspended sediment in Lick Creek, with the largest source being construction sites (Voli et al., 2013). This suggests the model may be overpredicting the sediment contribution from channel erosion. This could indicate the estimate of bank τ_c is too low, the clay bed material in the watershed is not as widespread or easily erodible as was assumed, or the model is overestimating knickpoint erosion. Bank erosion contributed < 10% of the modeled loading in all three simulations, suggesting that if any source is being overestimated, it is cohesive bed erosion and knickpoint migration. Alternatively, loading estimates may be accurate and the model could be overestimating the proportion that reaches the watershed outlet by neglecting fine sediment storage. Regardless, the simulations indicate that a significant amount of sediment could come from channel erosion, but that this would contribute very little phosphorus to the watershed. Importantly, the simulations do not show a significant decreasing trend in predicted loading, indicating that the channel will not adjust to a new stable state in the next 40 years and will instead continue to erode and be a source of fine sediment pollution.

The fact that upstream sediment supply has such a pronounced impact on modeled fine sediment loading illustrates the importance of accounting for altered sediment regimes in geomorphic and water quality analyses (Bledsoe, 2001; Wohl et al., 2015). Still, even the high sediment supply simulation (Q_s = 1.0) had significant fine sediment loading because knickpoint erosion — which is not impacted by incoming sediment loads — was a major loading source. Modeled loading in watersheds without knickpoints may be even more sensitive to supplied bed material from upstream. In reality, large sand and gravel loads could bury a migrating knickpoint; however, REM does not capture this behavior because the model assumes that as the knickpoint migrates, the height does not change.

5.2. Uncertainty in model projections

Uncertainty in loading estimates is high and it is important to put these results into perspective. Is this magnitude of uncertainty expected for loading estimates from channel erosion? Unfortunately, very few studies have quantified uncertainty in estimated pollutant loading in eroding streams. Purvis et al. (2016) quantified historic phosphorus loading from bank erosion using aerial imagery and measured bank P content. They estimated historic total P loading averaged 12,000 kg/yr (300–50,000 90% CI). The magnitude of loading is higher than model estimates for Big Dry Creek or Lick Creek, but the uncertainty range is similar. The Purvis et al. (2016) range was about four times their average estimate, lower than Big Dry Creek (range 6.3 times the median estimate) but higher than Lick Creek (range three times the median). Uncertainty ranges of sediment loading over the same time period were about twice the average value (Purvis and Fox, 2016). Model results also showed the same or lower uncertainty in sediment loading (Big Dry Creek range 5.9 times the median, Lick Creek range 2.7 times the median). This is expected since phosphorus loading results have all the same uncertainty as sediment loading, with the added effect of variable bank phosphorus concentrations.

Klavon et al. (2017) used aerial imagery and BSTEM to estimate sediment loading over a 10 year period in two streams. Their uncertainty ranges for the aerial analysis were significant (10,100–80,700 ton sed/yr and 12,600–38,400 ton sed/yr for the two streams) but were smaller than their model estimates (303–177,000 ton sed/yr and 494–34,000 ton sed/yr for the two streams). The aerial imagery uncertainty ranges were about one to one and half times the average, while BSTEM ranges were around twice the average result. While this is a limited set of studies, it indicates that the magnitude of uncertainty in model estimates from this study is similar to what has been quantified by others for sediment and phosphorus loads from both aerial imagery methods and modeling. A more interesting question remains: how does uncertainty in loading from channel erosion compare to *other* sources of sediment and phosphorus pollution?

Mittelstet and Storm (2016) quantified legacy phosphorus inputs from a variety of sources in a large watershed in Oklahoma and Arkansas. Their estimated annual loading of 3350 ton P/yr (2840–3860 ton/yr 90% CI) had a much smaller uncertainty range than model results from this study (less than one third of their average estimate). Uncertainty in GIS-estimated loading from non-point sources in Scotland (median 486 kg P/yr; 250–750 kg/yr 90% CI) was similar to uncertainty in measured loads (Murdoch et al., 2005). Another simple watershed model predicted daily TP concentrations of around 0.3 mg/L (0.2–0.4 mg/L 95% CI) (Smith et al., 2005). Application of the generalized likelihood uncertainty estimation (GLUE) to the integrated catchment model of phosphorus (INCA-P) showed similar uncertainty ranges, on the order of 0.2 mg/L (Dean et al., 2009). Even models of wastewater treatment facilities can show significant uncertainty in predicted nutrient effluent concentrations (Sin et al., 2011). Modeled TP concentrations from Lick Creek were low (median 0.003 mg/L) but the uncertainty range was about three times this median value, larger than what was observed in these other studies.

These results suggest that model estimates for Big Dry Creek and Lick Creek — and other studies quantifying loading from bank erosion — have significantly higher uncertainty than estimates from other non-point sources. It is possible that channel erosion is subject to inherently greater uncertainty than other sources of pollution, or simply that the uncertainty analysis of Big Dry Creek and Lick Creek accounted for more contributing factors than these other studies. It is important to note that the uncertainty analysis in this study should be considered preliminary. Accurately quantifying variability in model inputs is an essential part of uncertainty quantification (Melching and Yoon, 1996). For many REM inputs, however, it was assumed that variables followed uniform distributions that ranged from 50% to 150% of the initial value. This may be overestimating input parameter variability, leading to a conservative estimate of model output uncertainty and could explain why these uncertainty estimates were larger than estimates from other studies. More detailed quantification of input variability would lead to more accurate estimates of model uncertainty (Byrd and Melching, 2005; Melching and Bauwens, 2001).

5.3. Management implications & future research

Model results suggest that channel erosion in both Big Dry Creek and Lick Creek is not a significant source of phosphorus, the primary pollutant of concern in both watersheds. For managers interested in reducing nutrient pollution in these watersheds, addressing channel erosion is likely not the most cost-effective solution. If reducing fine sediment pollution is a management goal, model results indicate that mitigating channel erosion could significantly affect total watershed loads. Beyond just providing estimates of total loading, REM also identifies what parts of the channel network are contributing most to water quality degradation. In Lick Creek, for example, modeling showed that eroding knickpoints were the primary contributor of fine sediment (Fig. 10), and installation of grade control structures or other management interventions at these locations has significant potential to reduce sediment loading.

REM has a number of potential applications beyond what was examined here. For example, the model could be used to predict how different watershed management options (e.g. stormwater controls that reduce discharge) and stream restoration strategies (e.g. bed and bank stabilization) may impact channel evolution and associated pollutant loading. Other researchers have used BSTEM (Simon et al., 2011; Langendoen et al., 2012; Klavon et al., 2017) and CONCEPTS (Langendoen, 2011; Enlow et al., 2018) to estimate the relative impact of different channel restoration strategies on bank erosion; however, these two models are usually applied at the reach scale. REM is easily run at the watershed scale and accounts for how restoration in one part of the watershed may impact channel response elsewhere. Importantly, REM can also run Monte Carlo simulations to quantify uncertainty in

pollutant loading estimates. Incorporating uncertainty into estimates of pollutant loading from channel erosion is essential (Klavon et al., 2017; Fox et al., 2016), and can help managers make better informed decisions (Pappenberger and Beven, 2006).

In this study, REM was used to simulate sediment and phosphorus loading from bank erosion; however, the model can also be used to estimate loading of many other sediment-bound pollutants. Streambanks can contain high concentrations of lead (Palumbo-Roe et al., 2012) and other metals (Domínguez et al., 2016) or even radioactive contaminants (Paridaens and Vanmarcke, 2001). Furthermore, bank erosion has been shown to contribute significant amounts of mercury (Rhoades et al., 2009) and nitrogen (Walter et al., 2007) to watersheds. Although much of the work on bank erosion as a pollutant source has focused on sediment and phosphorus (Fox et al., 2016), exploring its role in other water quality issues is important for protecting water resources.

6. Conclusions

Future sediment and phosphorus loading from channel erosion was modeled in two watersheds using a new watershed-scale model that simulates both channel bed and bank erosion. Model results show that channel erosion is likely only a minor phosphorus source in both watersheds (< 5% of historic phosphorus load/concentration). On the other hand, channel erosion may be a significant source of fine sediment pollution, ranging from 30% to > 100% of historic sediment loads (Big Dry Creek) and concentrations (Lick Creek). Uncertainty ranges on these estimates were high, meaning model results should not be considered exact forecasts of what will happen, but instead estimates of relative magnitudes of phosphorus and sediment loading (low and high in the study watersheds, respectively). Importantly, model simulations show no decreasing trends in pollutant loading, indicating that both Big Dry Creek and Lick Creek will continue to erode and supply fine sediment to their watersheds. Also, the fact that loading estimates for Lick Creek declined as upstream sediment supply increased underscores the need to consider alterations in both flow and sediment when analyzing channel evolution (Wohl et al., 2015; Bledsoe, 2001) — especially in streams prone to active incision. This is the first application of REM to project future sediment and phosphorus loading from channel erosion. Channel erosion's importance as a pollutant source is increasing in recognition (Fox et al., 2016), and more studies are attempting to quantify the magnitude of pollutant loading using field measurements (e.g. Purvis et al., 2016; Beck et al., 2018) and modeling (e.g. Langendoen et al., 2012; Klavon et al., 2017; Stryker et al., 2017). REM can be a powerful new tool to assess the significance of this pollutant source and aid in planning targeted remediation and restoration to reduce loading rates and improve water quality.

Declarations of interest

None.

Acknowledgments

This work was partially funded by the National Science Foundation, Integrative Graduate Education and Research Traineeship (IGERT) [Grant No. DBE-0966346] 'I-WATER: Integrated Water, Atmosphere, Ecosystems Education and Research Program' at Colorado State University. Additional funding was provided by the United States Environmental Protection Agency (USEPA) [grant RD835570]. Its contents are solely the responsibility of the grantee and do not necessarily represent the official view of the USEPA. Further, USEPA does not endorse the purchase of any commercial products or services mentioned in the publication. The Urban Drainage and Flood Control District and members of the Big Dry Creek Watershed Association provided funding for field work on Big Dry Creek. We are grateful to Travis Hardee and Travis Stroth who assisted with the field data collection. We also want to thank Peter Nelson for providing guidance on model development and Mazdak Arabi, Sara Rathburn, and two anonymous reviewers for constructive comments on the manuscript. Jane Clary and Sandi Wilbur were excellent resources on Big Dry Creek and Lick Creek, respectively. Bank phosphorus data from both watersheds and additional information on model application and results are available in the "Supplementary Material". The River Erosion Model (including all source code) is available at www.github.com/rodlammers/REM.

Appendix A. Supplementary data

Supplementary data to this article can be found online at https://doi.org/10.1016/j.jenvman.2018.12.074.

References

Agudelo, S.C., Nelson, N.O., Barnes, P.L., Keane, T.D., Pierzynski, G.M., 2011. Phosphorus adsorption and desorption potential of stream sediments and field soils in agricultural watersheds. J. Environ. Qual. 40, 144–152. https://doi.org/10.2134/jeq2010.0153.

Allen, P.M., Arnold, J.G., Auguste, L., White, J., Dunbar, J., 2018. Application of a simple headcut advance model for gullies. Earth Surf. Process. Landforms 43, 202–217. https://doi.org/10.1002/esp.4233.

Beck, W., Isenhart, T., Moore, P., Schilling, K., Schultz, R., Tomer, M., 2018. Streambank alluvial unit contributions to suspended sediment and total phosphorus loads, Walnut Creek, Iowa, USA. Water 10, 111. https://doi.org/10.3390/w10020111.

Biron, P.M., Choné, G., Buffin-Bélanger, T., Demers, S., Olsen, T., 2013. Improvement of streams hydro-geomorphological assessment using LiDAR DEMs. Earth Surf. Process. Landforms 38, 1808–1821. https://doi.org/10.1002/esp.3425.

Bledsoe, B.P., 2001. Relationships of stream responses to hydrologic changes. In: Urbonas, B.R. (Ed.), Linking Stormwater BMP Designs and Performance to Receiving Water Impact Mitigation. American Society of Civil Engineers, pp. 127–144. https://doi.org/10.1061/40602(263)10.

Bledsoe, B.P., O'Connor, K.A., Watson, C.C., Carlson, K.H., 2000. Phosphorus Content of Bed, Bank and Upland Sediments: Long Creek and Johnson Creek Watersheds, Mississippi. Technical Report Colorado State University: Prepared for USACE, Vicksburg District.

Bledsoe, B.P., Stein, E.D., Hawley, R.J., Booth, D., 2012. Framework and tool for rapid assessment of stream susceptibility to hydromodification. JAWRA J. Am. Water Resour. Assoc. 48, 788–808.

Booth, D.B., Fischenich, C.J., 2015. A channel evolution model to guide sustainable urban stream restoration. Area 47, 408–421. https://doi.org/10.1111/area.12180.

Byrd, J.L., Melching, C.S., 2005. Uncertainty evaluation in the design of instream structures for stream restoration. In: Proceedings of XXXI Congress of the International Association for Hydraulic Engineering and Research, pp. 2172–2182 (Seoul, Korea).

Clary, J., 2017. Big Dry Creek Annual Water Quality Summary for 2016. Technical Report Prepared for the Big Dry Creek Watershed Association by Wright Water Engineers, Inc. http://www.bigdrycreek.org/sg_cms/jscripts/tiny_mce/plugins/filemanager/files/BDC_Annual_Report_2017.pdf.

Cluer, B., Thorne, C., 2014. A stream evolution model integrating habitat and ecosystem benefits. River Res. Appl. 30, 135–154. https://doi.org/10.1002/rra.

Collins, A.L., Walling, D.E., 2007. Sources of fine sediment recovered from the channel bed of lowland groundwater-fed catchments in the UK. Geomorphology 88, 120–138. https://doi.org/10.1016/j.geomorph.2006.10.018.

Cooper, J.R., Gilliam, J.W., 1987. Phosphorus redistribution from cultivated fields into riparian areas. Soil Sci. Soc. Am. J. 51, 1600–1604. https://dl.sciencesocieties.org/publications/sssaj/abstracts/51/6/SS0510061600.

Dean, S., Freer, J., Beven, K.J., Wade, A.J., Butterfield, D., 2009. Uncertainty assessment of a process-based integrated catchment model of phosphorus. Stoch. Environ. Res. Risk Assess. 23, 991–1010. https://doi.org/10.1007/s00477-008-0273-z.

Domínguez, M.T., Alegre, J.M., Madejón, P., Madejón, E., Burgos, P., Cabrera, F., Marañón, T., Murillo, J.M., 2016. River banks and channels as hotspots of soil pollution after large-scale remediation of a river basin. Geoderma 261, 133–140. https://doi.org/10.1016/j.geoderma.2015.07.008.

Enlow, H.K., Fox, G.A., Boyer, T.A., Stoecker, A., Storm, D.E., Starks, P., Guertault, L., 2018. A modeling framework for evaluating streambank stabilization practices for reach-scale sediment reduction. Environ. Model. Software 100, 201–212. https://doi.org/10.1016/j.envsoft.2017.11.010.

Fox, G.A., Purvis, R.A., Penn, C.J., 2016. Streambanks: a net source of sediment and phosphorus to streams and rivers. J. Environ. Manag. 181, 602–614. https://doi.org/10.1016/j.jenvman.2016.06.071.

Gibson, S., Simon, A., Langendoen, E.J., Bankhead, N., Shelley, J., 2015. A physically-based channel-modeling framework integrating HEC-RAS sediment transport capabilities and the USDA-ARS Bank-Stability and Toe-Erosion Model (BSTEM). In: 3rd Joint Federal Interagency Sedimentation and Hydrologic Modeling Conference. NV, Reno, pp. 12.

Google Earth Pro, 2017. Google Earth Imagery.

Haggard, B.E., Smith, D.R., Brye, K.R., 2007. Variations in stream water and sediment phosphorus among select Ozark catchments. J. Environ. Qual. 36, 1725–1734. https://doi.org/10.2134/jeq2006.0517.

Homer, C.G., Dewitz, J.A., Yang, L., Jin, S., Danielson, P., Xian, G., Coulston, J., Herold, N.D., Wickham, J.D., Megown, K., 2015. Completion of the 2011 National Land Cover Database for the conterminous United States - representing a decade of land

cover change information. Photogramm. Eng. Rem. Sens. 81, 345–354.
Howe, E., Winchell, M., Meals, D., Folle, S., Moore, J., Braun, D., DeLeo, C., Budreski, K., Schiff, R., 2011. Identification of Critical Source Areas of Phosphorus within the Vermont Sector of the Missisquoi Bay Basin. Technical Report Stone Environmental Inc Prepared for Lake Champlain Basin Program, Grand Isle, VT.
Ishee, E.R., Ross, D.S., Garvey, K.M., Bourgault, R.R., Ford, C.R., 2015. Phosphorus characterization and contribution from eroding streambank soils of Vermont's Lake Champlain basin. J. Environ. Qual. 44, 1745–1753. https://doi.org/10.2134/jeq2015.02.0108.
Kerr, J.G., Burford, M., Olley, J., Udy, J., 2011. Phosphorus sorption in soils and sediments: implications for phosphate supply to a subtropical river in southeast Queensland, Australia. Biogeochemistry 102, 73–85. https://doi.org/10.1007/s10533-010-9422-9.
Klavon, K., Fox, G., Guertault, L., Langendoen, E., Enlow, H., Miller, R., Khanal, A., 2017. Evaluating a process-based model for use in streambank stabilization: insights on the bank stability and toe erosion model (BSTEM). Earth Surf. Process. Landforms 42, 191–213. https://doi.org/10.1002/esp.4073.
Kronvang, B., Audet, J., Baattrup-Pedersen, A., Jensen, H.S., Larsen, S.E., 2012. Phosphorus load to surface water from bank erosion in a Danish lowland river basin. J. Environ. Qual. 41, 304–313. https://doi.org/10.2134/jeq2010.0434. http://www.ncbi.nlm.nih.gov/pubmed/22370392.
Kronvang, B., Grant, R., Laubel, A., 1997. Sediment and phosphorus export from a lowland catchment: quantification of sources. Water Air Soil Pollut. 99, 465–476.
Lammers, R.W., 2018. Modeling Stream Evolution and its Consequences for Watershed Scale Pollutant Loading. Phd dissertation Colorado State University.
Lammers, R.W., Bledsoe, B.P., 2017. What role does stream restoration play in nutrient management? Crit. Rev. Environ. Sci. Technol. 47, 335–371. https://doi.org/10.1080/10643389.2017.1318618.
Lammers, R.W., Bledsoe, B.P., 2018a. A network scale, intermediate complexity model for simulating channel evolution over years to decades. J. Hydrol. 566, 886–900. https://doi.org/10.1016/j.jhydrol.2018.09.036.
Lammers, R.W., Bledsoe, B.P., 2018b. Parsimonious sediment transport equations based on Bagnold's stream power approach for river modeling and management. Earth Surf. Process. Landforms 43, 242–258. https://doi.org/10.1002/esp.4237.
Langendoen, E.J., 2011. Application of the CONCEPTS channel evolution model in stream restoration strategies. Geophys. Monogr. 487–502. http://www.agu.org/books/gm/v194/2010GM000986/2010GM000986.shtml.
Langendoen, E.J., Simon, A., 2008. Modeling the evolution of incised streams: II. Streambank erosion. J. Hydraul. Eng. 134, 905–915.
Langendoen, E.J., Simon, A., Klimetz, L., Bankhead, N., Ursic, M.E., 2012. Quantifying Sediment Loadings from Streambank Erosion in Selected Agricultural Watersheds Draining to Lake Champlain. Technical Report 72 U.S. Department of Agriculture - Agricultural Research Service National Sedimentation Laboratory Watershed Physical Processes Research Unit Oxford, MS.
Melching, C.S., Bauwens, W., 2001. Uncertainty in coupled nonpoint source and stream water-quality models. J. Water Resour. Plann. Manag. 127, 403–413.
Melching, C.S., Yoon, C.G., 1996. Key sources of uncertainty in QUAL2E model of Passaic River. J. Water Resour. Plann. Manag. 122, 105–113.
Midgley, T.L., Fox, G.A., Heeren, D.M., 2012. Evaluation of the bank stability and toe erosion model (BSTEM) for predicting lateral retreat on composite streambanks. Geomorphology 145–146, 107–114. https://doi.org/10.1016/j.geomorph.2011.12.044.
Miller, R.B., Fox, G.A., Penn, C.J., Wilson, S., Parnell, A., Purvis, R.A., Criswell, K., 2014. Estimating sediment and phosphorus loads from streambanks with and without riparian protection. Agric. Ecosyst. Environ. 189, 70–81.
Mittelstet, A., Storm, D., Fox, G., 2016. Testing of the modified streambank erosion and instream phosphorus routines for the SWAT model. JAWRA J. Am. Water Resour. Assoc. 1–14. https://doi.org/10.1111/1752-1688.12485.
Mittelstet, A.R., Storm, D.E., 2016. Quantifying legacy phosphorus using a mass balance approach and uncertainty analysis. J. Am. Water Resour. Assoc. 52, 1297–1310. https://doi.org/10.1111/1752-1688.12453.
Murdoch, E.G., Whelan, M.J., Grieve, I.C., 2005. Incorporating uncertainty into predictions of diffuse-source phosphorus transfers (using readily available data). Water Sci. Technol. 51, 339–346.
Nellesen, S.L., Kovar, J.L., Haan, M.M., Russell, J.R., 2011. Grazing management effects on stream bank erosion and phosphorus delivery to a pasture stream. Can. J. Soil Sci. 91, 385–395. https://doi.org/10.4141/CJSS10006.
North Carolina Department of Environmental Quality, 2016. Draft 2016 Category 5 Assessments EPA Submittal - 303(d) List. https://files.nc.gov/ncdeq/WaterQuality/Planning/TMDL/303d/2016/NC_2016_Category_5_20160606.pdf.
Palmer, J.A., Schilling, K.E., Isenhart, T.M., Schultz, R.C., Tomer, M.D., 2014. Streambank erosion rates and loads within a single watershed: bridging the gap between temporal and spatial scales. Geomorphology 209, 66–78. https://doi.org/10.1016/j.geomorph.2013.11.027.
Palmer-Felgate, E.J., Jarvie, H.P., Withers, P.J.A., Mortimer, R.J.G., Krom, M.D., 2009. Stream-bed phosphorus in paired catchments with different agricultural land use intensity. Agric. Ecosyst. Environ. 134, 53–66. https://doi.org/10.1016/j.agee.2009.05.014.
Palumbo-Roe, B., Wragg, J., Banks, V.J., 2012. Lead mobilisation in the hyporheic zone and river bank sediments of a contaminated stream: contribution to diffuse pollution. J. Soils Sediments 12, 1633–1640. https://doi.org/10.1007/s11368-012-0552-7.
Pappenberger, F., Beven, K.J., 2006. Ignorance is bliss: or seven reasons not to use uncertainty analysis. Water Resour. Res. 42, 1–8. https://doi.org/10.1029/2005WR004820. arXiv:‘.
Paridaens, J., Vanmarcke, H., 2001. Radium contamination of the banks of the River Laak as a consequence of the phosphate industry in Belgium. J. Environ. Radioact. 54, 53–60. https://doi.org/10.1016/S0265-931X(00)00165-X.
Partheniades, E., 1965. Erosion and deposition of cohesive soils. J. Hydraul. Div. 91, 105–139.
Peacher, R., 2011. Impacts of Land Use on Stream Bank Erosion in the Northeast Missouri Claypan Region. Master’s thesis. Iowa State University.
Plischke, E., Borgonovo, E., Smith, C.L., 2013. Global sensitivity measures from given data. Eur. J. Oper. Res. 226, 536–550. https://doi.org/10.1016/j.ejor.2012.11.047.
Purvis, R.A., Fox, G.A., 2016. Streambank sediment loading rates at the watershed scale and the benefits of riparian protection. Earth Surf. Process. Landforms. https://doi.org/10.1002/esp.3901.
Purvis, R.A., Fox, G.A., Penn, C.J., Storm, D.E., Parnell, A., 2016. Estimating streambank phosphorus loads at the watershed scale with uncertainty analysis approach. J. Hydrol. Eng. 21, 04016028. https://doi.org/10.1061/(ASCE)HE.1943-5584.0001402.
R Core Team, 2018. R: a Language and Environment for Statistical Computing. R Foundation for Statistical Computing, Vienna, Austria.
Rhoades, E.L., O'Neal, M.A., Pizzuto, J.E., 2009. Quantifying bank erosion on the South River from 1937 to 2005, and its importance in assessing Hg contamination. Appl. Geogr. 29, 125–134. https://doi.org/10.1016/j.apgeog.2008.08.005.
Schumm, S.A., Harvey, M.D., Watson, C.C., 1984. Incised Channels: Morphology, Dynamics and Control. Water Resources Publications, Littleton, CO.
Simon, A., 1989. A model of channel response in disturbed alluvial channels. Earth Surf. Process. Landforms 14, 11–26.
Simon, A., Curini, A., Darby, S.E., Langendoen, E.J., 2000. Bank and near-bank processes in an incised channel. Geomorphology 35, 193–217. https://doi.org/10.1016/S0169-555X(00)00036-2.
Simon, A., Pollen-Bankhead, N., Thomas, R.E., 2011. Development and application of a deterministic bank stability and toe erosion model for stream restoration. In: Simon, A., Bennett, S., Castro, J. (Eds.), Stream Restoration in Dynamic Fluvial Systems: Scientific Approaches, Analyses, and Tools. American Geophysical Union, Washington, D.C., pp. 453–474.
Simon, A., Thomas, R.E., Klimetz, L., 2010. Comparison and experiences with field techniques to measure critical shear stress and erodibility of cohesive deposits. In: 2nd Joint Federal Interagency Conference, Las Vegas, pp. 826.
Sin, G., Gernaey, K.V., Neumann, M.B., van Loosdrecht, M.C., Gujer, W., 2011. Global sensitivity analysis in wastewater treatment plant model applications: prioritizing sources of uncertainty. Water Res. 45, 639–651. https://doi.org/10.1016/j.watres.2010.08.025.
Smith, D.B., Cannon, W.F., Woodruff, L.G., Solano, F., Kilburn, J.E., Fey, D.L., 2013. Geochemical and mineralogical data for soils of the conterminous United States. Technical Report U.S. Geological Survey Data Series 801.
Smith, R.M., Evans, D.J., Wheater, H.S., 2005. Evaluation of two hybrid metric-conceptual models for simulating phosphorus transfer from agricultural land in the River Enborne, a lowland UK catchment. J. Hydrol. 304, 366–380. https://doi.org/10.1016/j.jhydrol.2004.07.046.
Stryker, J., Wemple, B., Bomblies, A., 2017. Modeling sediment mobilization using a distributed hydrological model coupled with a bank stability model. Water Resour. Res. 53, 2051–2073. https://doi.org/10.1002/2013WR014979.Reply. arXiv:2014WR016527.
Thoma, D.P., Gupta, S.C., Bauer, M.E., Kirchoff, C.E., 2005. Airborne laser scanning for riverbank erosion assessment. Rem. Sens. Environ. 95, 493–501. https://doi.org/10.1016/j.rse.2005.01.012.
Tufekcioglu, M., 2010. Stream Bank Soil and Phosphorus Losses within Grazed Pasture Stream Reaches in the Rathbun Watershed in Southern Iowa. Phd dissertation Iowa State University.
U.S. EPA, 2015. Watershed Assessment, Tracking & Environmental Results. National Summary of State Information. http://ofmpub.epa.gov/waters10/attains_nation_cy.control.
Voli, M.T., Wegmann, K.W., Bohnenstiehl, D.R., Leithold, E., Osburn, C.L., Polyakov, V., 2013. Fingerprinting the sources of suspended sediment delivery to a large municipal drinking water reservoir: Falls Lake, Neuse River, North Carolina, USA. J. Soils Sediments 13, 1692–1707. https://doi.org/10.1007/s11368-013-0758-3.
Walter, R., Merritts, D., Rahnis, M., 2007. Estimating Volume, Nutrient Content, and Rates of Stream Bank Erosion of Legacy Sediment in the Piedmont and Valley and Ridge Physiographic Provinces. Technical Report Report to the Pennsylvania Department of Environmental Protection. http://www.education.state.pa.us/portal/server.pt/gateway/PTARGS_0_2_900102_0_0_18/padeplegacysedimentreport2007waltermerrittsrahnisfinal.pdf.
Wohl, E.E., Bledsoe, B.P., Jacobson, R.B., Poff, N.L., Rathburn, S.L., Walters, D.M., Wilcox, A.C., 2015. The natural sediment regime in rivers: broadening the foundation for ecosystem management. Bioscience 65, 358–371. https://doi.org/10.1093/biosci/biv002.
Young, E.O., Ross, D.S., Alves, C., Villars, T., 2012. Soil and landscape influences on native riparian phosphorus availability in three Lake Champlain Basin stream corridors. J. Soil Water Conserv. 67, 1–7. https://doi.org/10.2489/jswc.67.1.1.
Zaimes, G.N., Schultz, R.C., Isenhart, T.M., 2008. Streambank soil and phosphorus losses under different riparian land-uses in Iowa. J. Am. Water Resour. Assoc. 44, 935–947. https://doi.org/10.1111/j.1752-1688.2008.00210.x.

Supplementary Material for "Modeling watershed phosphorus and sediment loading from river erosion while accounting for uncertainty"

Roderick W. Lammers and Brian P. Bledsoe

1 Model Calibration

1.1 Critical Shear Stress Calibration

We calibrated critical shear stress values for bank material using measured historic erosion rates and estimates of applied stream power over the period of observation. We calculated stream power using 15-min and hourly gage data (whichever was available) and converted them to a bank or wall shear stress using the same empirical equation used by REM:

$$\tau_w = 0.83\omega^{0.65} \tag{1}$$

where τ_w is the shear stress acting on the channel bank [Pa] and ω is specific stream power [W m^{-2}]. We then calculated fluvial erosion using the excess shear stress equation:

$$E = k\Delta t(\tau - \tau_c) \tag{2}$$

where E is eroded distance [m], Δt is the time step, τ_c is the critical shear stress of the bank material [Pa], and k is the erodibility of the bank material [m^3 N^{-1} s^{-1}] which was calculated as (*Simon et al.*, 2010):

$$k = 1.6 \times 10^{-6}\tau_c^{-0.826} \tag{3}$$

We calculated the value of τ_c that resulted in the best match between measured and calculated erosion rates (Figure S1). For Big Dry Creek, all erosion measurements were located on channel bends. Therefore, we adjusted the value of τ_w to account for higher shear stress on the outside of bends (*Army Corps of Engineers*, 1970):

$$\tau_{max} = 2.65\tau_w \left(\frac{R_c}{w}\right)^{-1/2} \tag{4}$$

where R_c is the bend radius of curvature [m] (estimated from aerial imagery) and w is channel width.

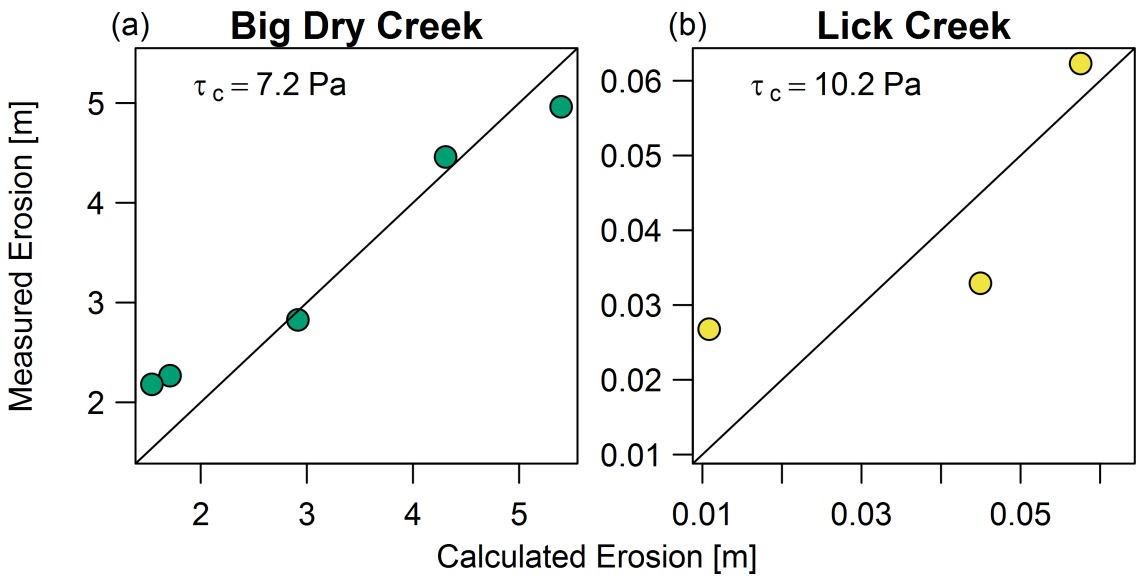

Figure S1: Measured versus predicted erosion distance for the calibrated value of τ_c for Big Dry Creek (a) and Lick Creek (b). The Big Dry Creek data are from five different locations over the same time period (1993 – 2014). The Lick Creek data are actually from nearby Ellerbe Creek at one location for three time periods (annually from 2014 – 2017).

1.2 Knickpoint Calibration

During the field data collection in Lick Creek, we identified two active knickpoints. These knickpoints were later located on the 2015 DEM and a 10 ft resolution DEM from 2001. We calculated a value of K_d from the knickpoint migration model that matched the observed migration rate over this time period. Calibrated values of K_d were 0.253 cm/Pa/s and 0.219 cm/Pa/s. Observed migration rates of the two knickpoints were 26.8 m/yr and 10.1 m/yr. Normalized to their watershed area gives rates of 4.12 m/km^2/yr and 1.64 m/km^2/yr, respectively. These normalized rates are within the ranges observed in Mississippi streams (median 0.83, range 0.03 – 5.43 m/km^2/yr) (*Jaeger et al.*, 2010).

1.3 Bank Cohesion Calibration

Figure S2 shows the data and fitted logistic regression model for predicting bank stability in Big Dry Creek and Lick Creek.

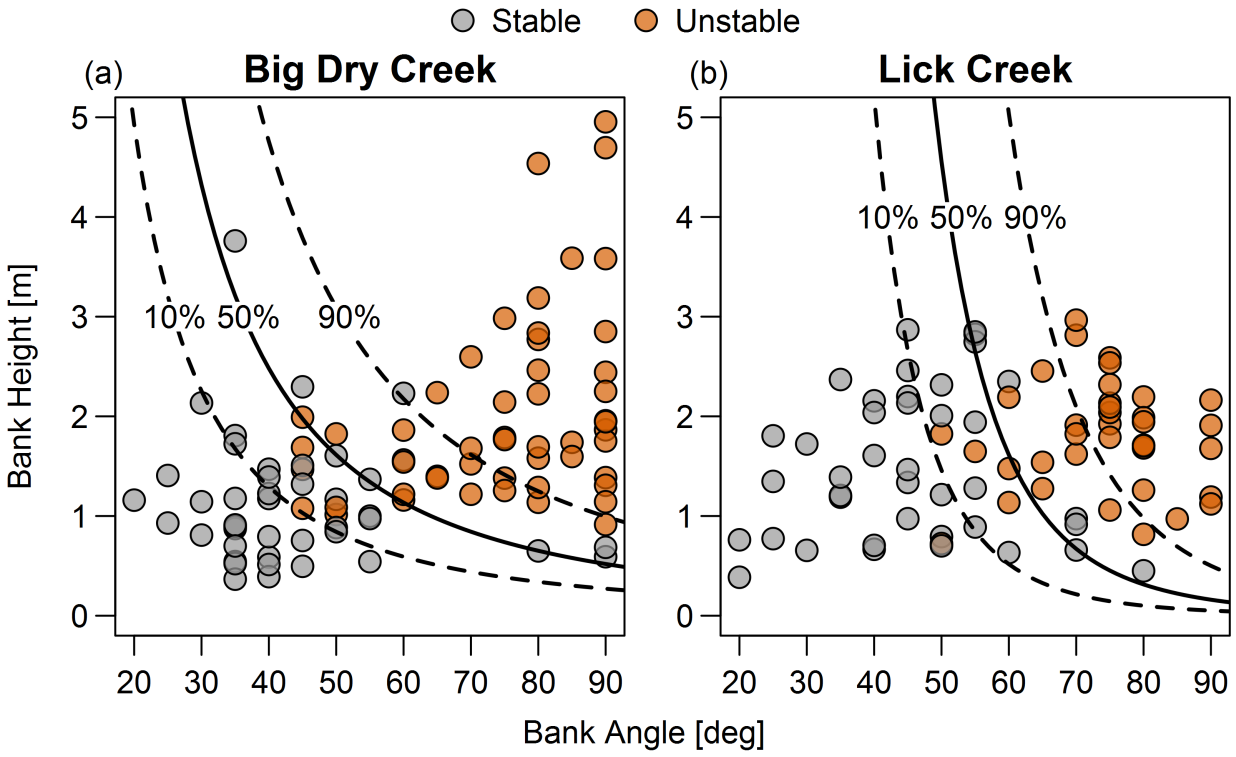

Figure S2: Measured bank heights and angles for stable and unstable banks and fitted logistic regression for predicting bank stability for Big Dry Creek (a) and Lick Creek (b). Percentages are probabilities of bank failure.

2 Watershed Population Estimates

Historic population densities for Big Dry Creek and Lick Creek (and its adjacent watershed, Little Lick Creek) were estimated from census block population data (*Manson et al.*, 2017). These population data were scaled based on the proportion of each census block within the watershed boundary (*Rosburg et al.*, 2017). The population of Big Dry Creek has increased steadily since 1970 (Figure S3). Recent population growth in Lick Creek mirrors growth in Little Lick Creek from 1980 – 1990, the period for which discharge data from Little Lick Creek were available.

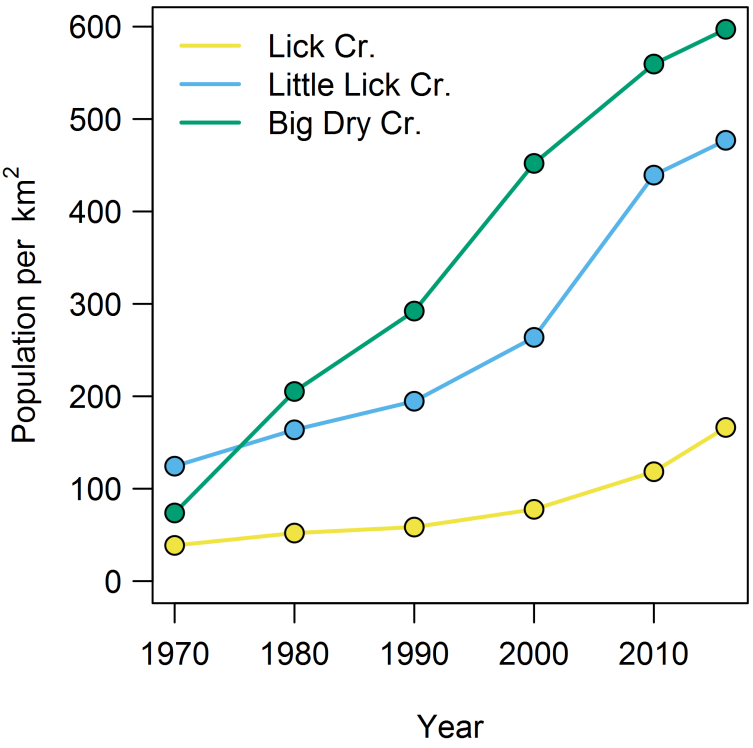

Figure S3: Population density estimates for the three watersheds from 1970 – 2016.

3 Model Inputs

Tables S1 and S2 summarize model inputs for both Big Dry Creek and Lick Creek.

Table S1: Big Dry Creek model inputs.

Variable	**Value**	**MC Values**	**Source**
Bed profile	–	–	LiDAR DEM
Bank geometry	0.9 – 2 m; 45° – 90°	±50%[1]	Field measured
Width [m]	5 – 7	±50%[1]	LiDAR DEM
Discharge	–	–	See text
Sediment supply	50% and 100% of transport capacity	–	Assumed
Bank τ_c [Pa]	7.2	±50%[1]	Calibrated
Bank cohesion [kPa]	1.4	normal (mean = 1.4; sd = 0.4)	Calculated from bank geometry
Bank friction angle, ϕ' [deg]	22	±50%[1]	Typical values (*Simon et al.*, 2011)
Bank soil weight [kN/m^3]	18	±50%[1]	Typical values (*Simon et al.*, 2011)
Bank P [mg/kg]	310	normal (mean = 310; sd = 100)	Measured
Bank bedload prop[2]	38 – 64%	±50%[1]	% Sand from sampled banks
Cohesive bed	5 grade control structures	–	Field observations
GSD	D_{50} = 2 mm; σ_g = 1.5	±50%[1]	Assumed
Floodplain geometry	width: 50 m; slope: 1°	±50%[1]	Assumed
Manning n	chnl: 0.035; fp: 0.06	±50%[1]	Assumed
R_c [m]	35	±50%[1]	Aerial imagery
Sinuosity	1.3 – 2.4	±50%[1]	Aerial imagery

[1]Uniform distribution.
[2]Proportion of the eroded bank material that is bed material load (sand and coarser). The remainder is assumed to be washload.

Table S2: Lick Creek model inputs.

Variable	**Value**	**MC Values**	**Source**
Bed profile	–	–	LiDAR DEM
Bank geometry	1 – 2.8 m; 48° – 70°	±50%[1]	Field measured
Width [m]	1.8 – 17.3	±50%[1]	LiDAR DEM
Discharge	–	–	See text
Sediment supply	50% - 100% of transport capacity	–	Assumed
Bank τ_c [Pa]	10.2	±50%[1]	Calibrated
Bank cohesion [kPa]	2.1	lognormal (logmean = 0.44; logsd = 0.78)	Calculated from bank geometry
Bank friction angle, ϕ' [deg]	22	±50%[1]	Typical values (*Simon et al.*, 2011)
Bank soil weight [kN/m^3]	18	±50%[1]	Typical values (*Simon et al.*, 2011)
Bank P [mg/kg]	50	normal (mean = 53; sd = 30)	Measured
Bank bedload prop[2]	28 – 59%	±50%[1]	% Sand from sampled banks
Cohesive bed	0 – 2 m depth; τ_c = 10.2 Pa	–	Field observations; assumed τ_c = bank
D_{50}	uniform 2 mm	0.5 – 3.5 mm	Assumed
Floodplain geometry	width: 40 – 160 m; slope: 2° – 8°	±50%[1]	LiDAR DEM
Manning n	chnl: 0.045; fp: 0.08	±50%[1]	Assumed
Knickpoints	height: 0.9 – 1.3 m; K_d: 0.219 – 0.253 cm/Pa/hr	–	LiDAR DEM & Field observations

[1]Uniform distribution.
[2]Proportion of the eroded bank material that is bed material load (sand and coarser). The remainder is assumed to be washload.

4 Watershed Photographs

Figures S4 and S5 show representative photographs of stream channels in the Big Dry Creek and Lick Creek watersheds.

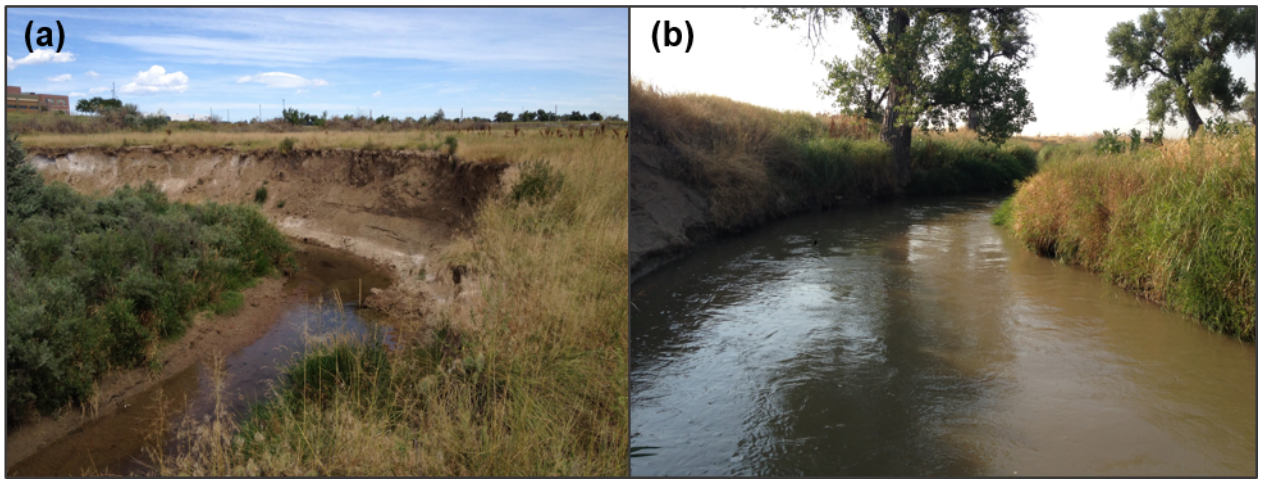

Figure S4: Looking upstream at an incised and actively migrating channel in the middle portion of the Big Dry Creek watershed (a); eroding bank height about 5 m. Looking downstream at a less incised and less laterally active portion of the channel near the watershed outlet (b); left bank height about 1.2 m. Photo taken August 2015.

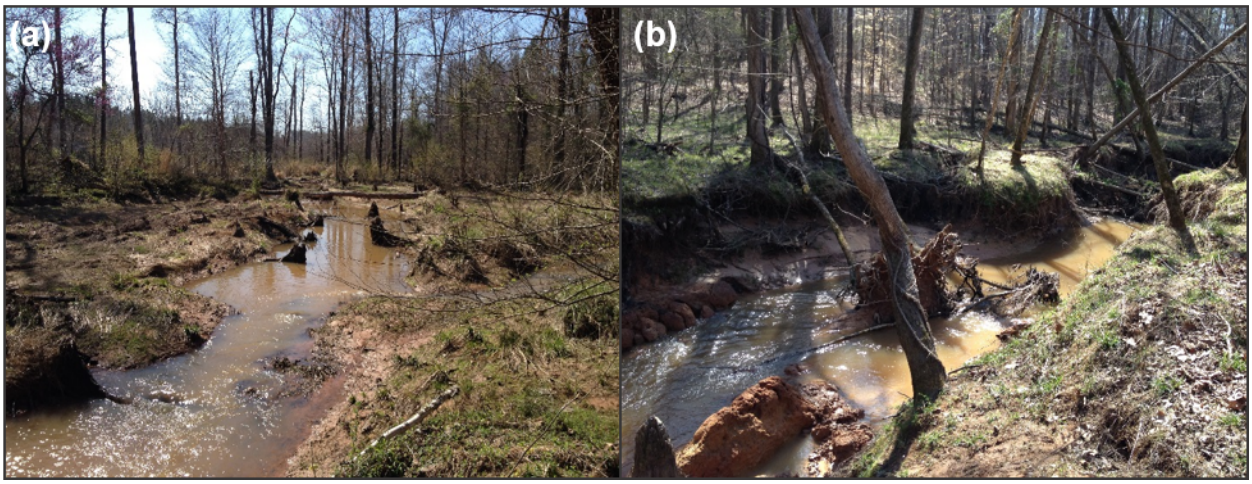

Figure S5: A tributary to Lick Creek immediately upstream (a) and downstream (b) of a 1 m high knickpoint. Both photographs are looking upstream. The channel downstream of the knickpoint is much deeper and wider than the upstream channel. Photo taken March 2016.

5 Additional Model Results

5.1 Big Dry Creek, $Q_s = 0.5$

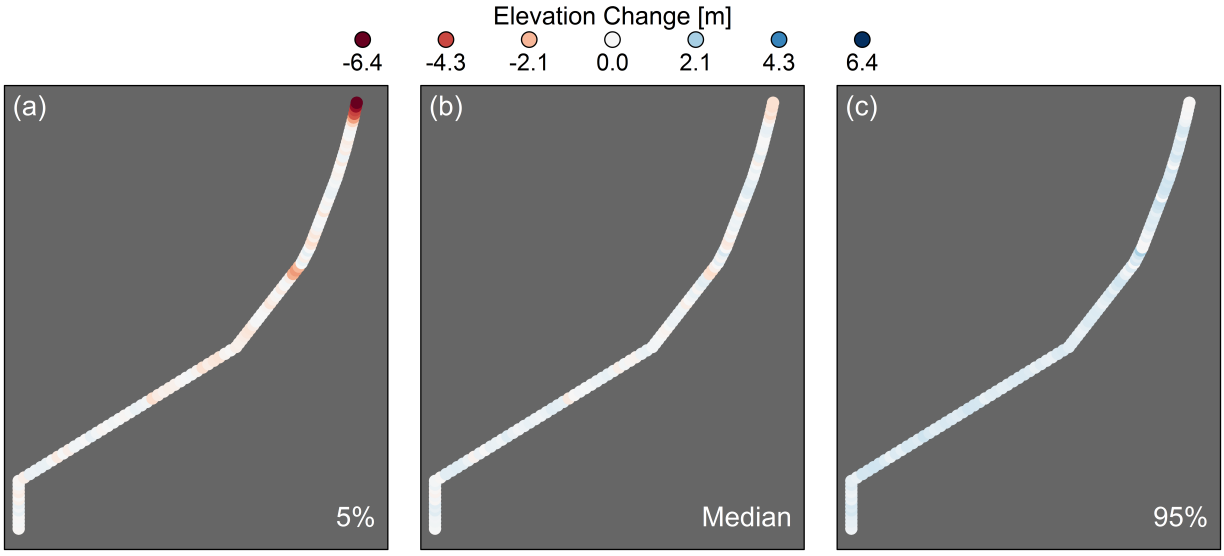

Figure S6: Changes in bed elevation throughout the Big Dry Creek drainage basin, including the median results and 5^{th} and 95^{th} percentiles. Model runs with $Q_s = 0.5$ transport capacity.

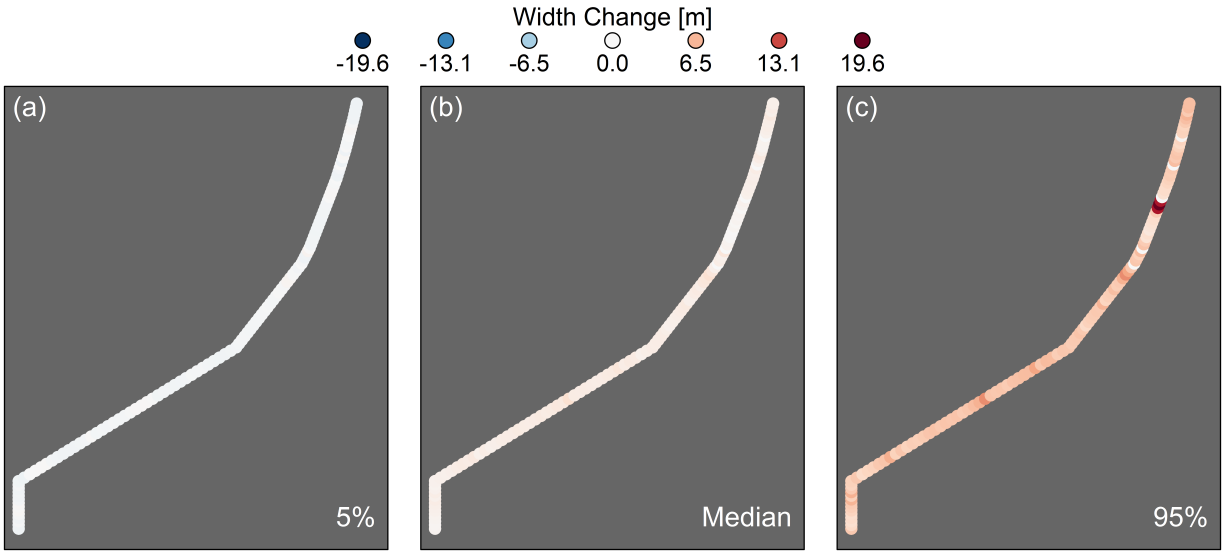

Figure S7: Changes in channel width throughout the Big Dry Creek drainage basin, including the median results and 5^{th} and 95^{th} percentiles. Model runs with $Q_s = 0.5$ transport capacity.

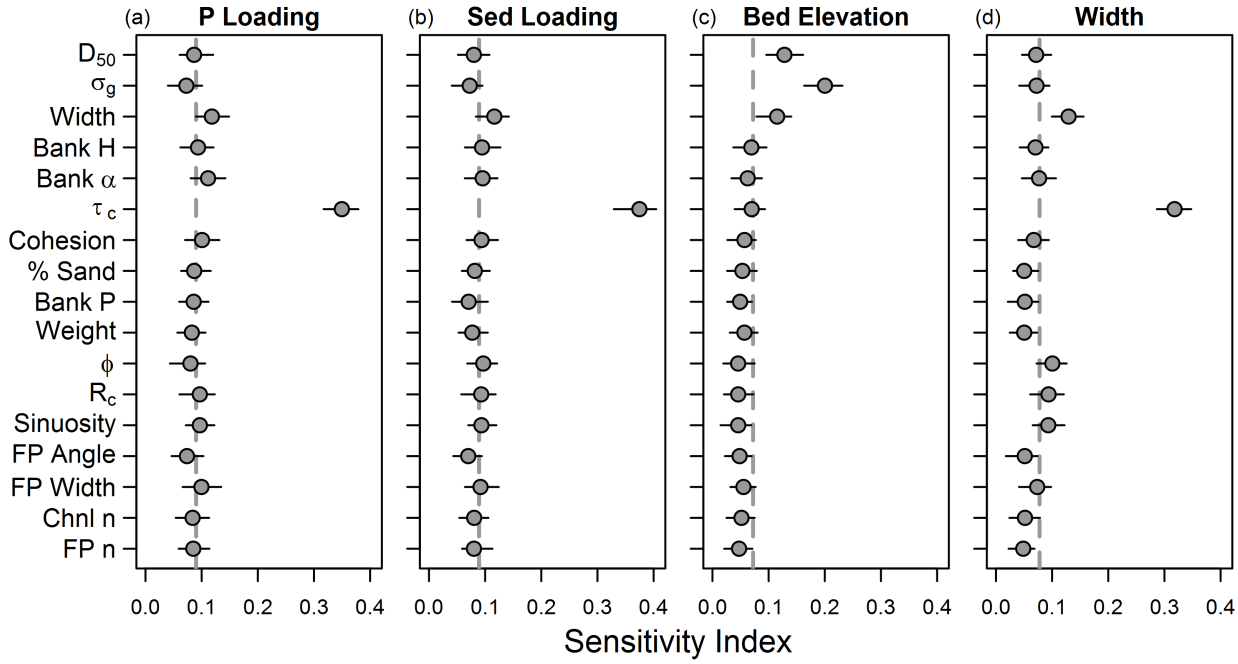

Figure S8: Big Dry Creek sensitivity analysis results for four different model outputs: phosphorus loading (a), sediment loading (b), bed elevation (c), and channel width (d). Points show bias-corrected sensitivity indices with ranges of estimates from bootstrapping. Points below the vertical dashed line had no influence on model output. Results from model runs with $Q_s = 0.5$ transport capacity.

5.2 Big Dry Creek, $Q_s = 1.0$

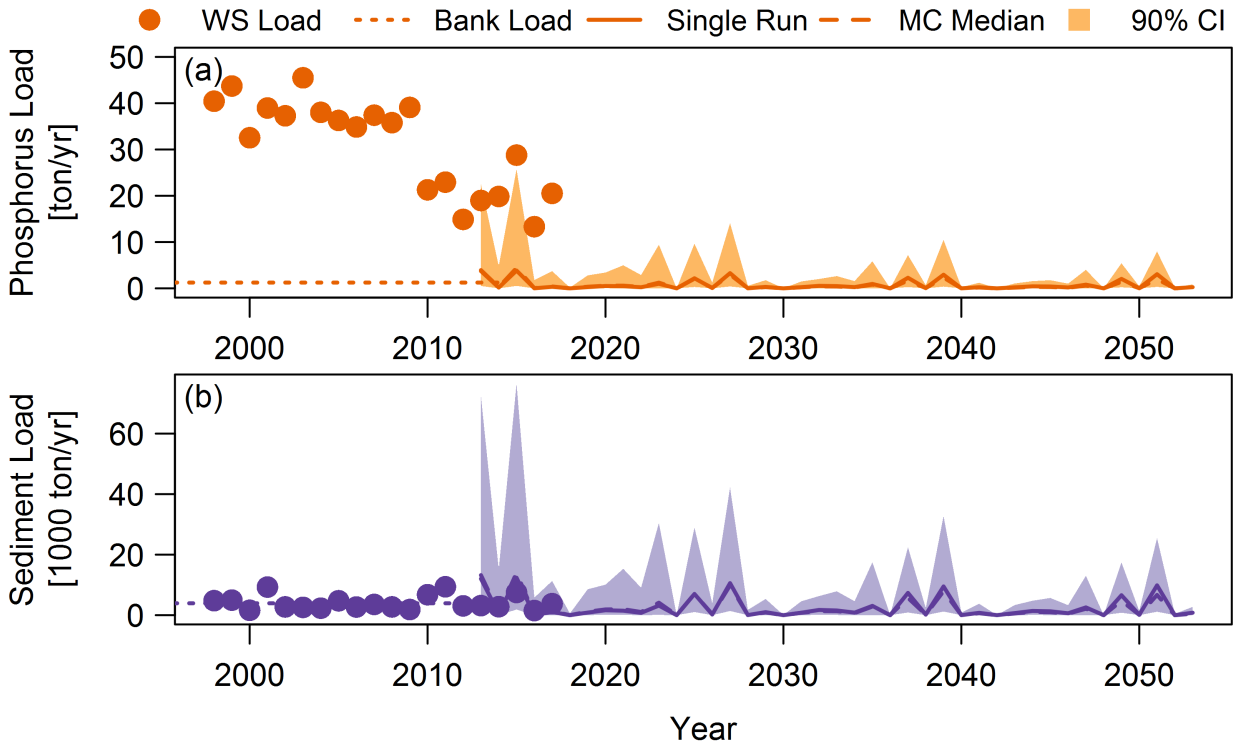

Figure S9: Observed and modeled average annual loads of phosphorus (a) and sediment (b) in Big Dry Creek. Measured watershed loads are shown as points, bank loading estimates from the aerial photo analysis are shown as a horizontal dotted line, and model results for the single model run (solid line), median of the Monte Carlo simulations (dashed line), and 90% CI are projected through 2053. Model results are from simulations with $Q_s = 1.0$ transport capacity.

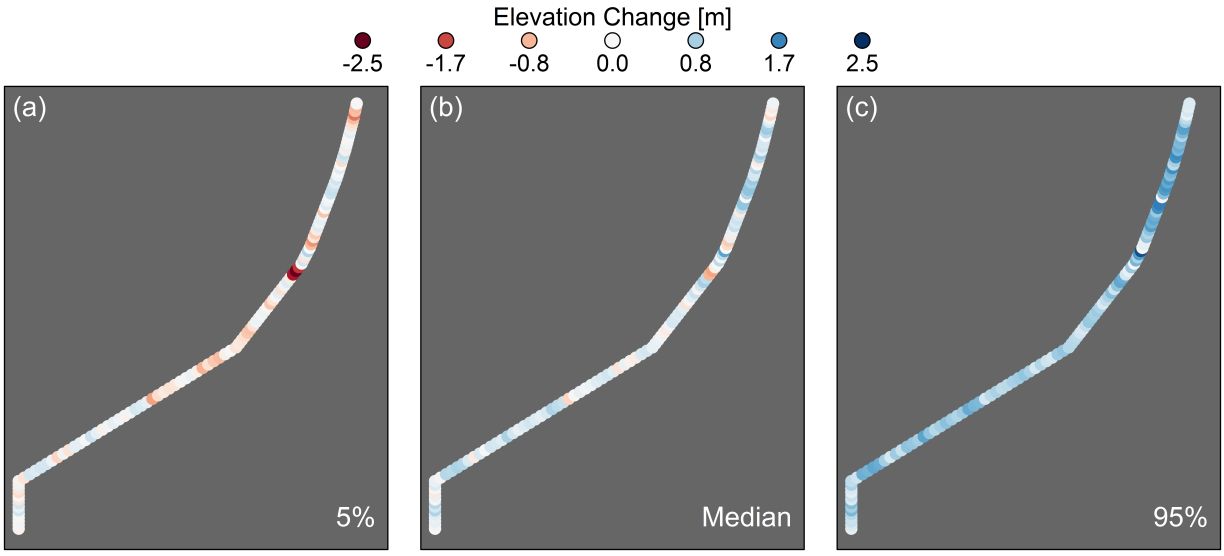

Figure S10: Changes in bed elevation throughout the Big Dry Creek drainage basin, including the median results and 5^{th} and 95^{th} percentiles. Model runs with $Q_s = 1.0$ transport capacity.

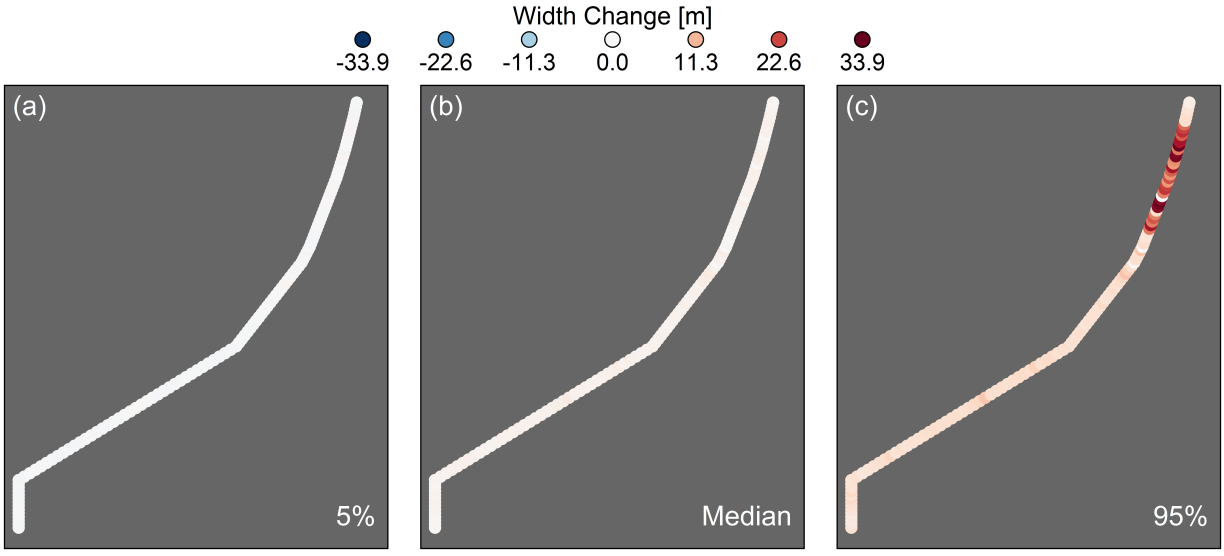

Figure S11: Changes in channel width throughout the Big Dry Creek drainage basin, including the median results and 5^{th} and 95^{th} percentiles. Model runs with $Q_s = 1.0$ transport capacity.

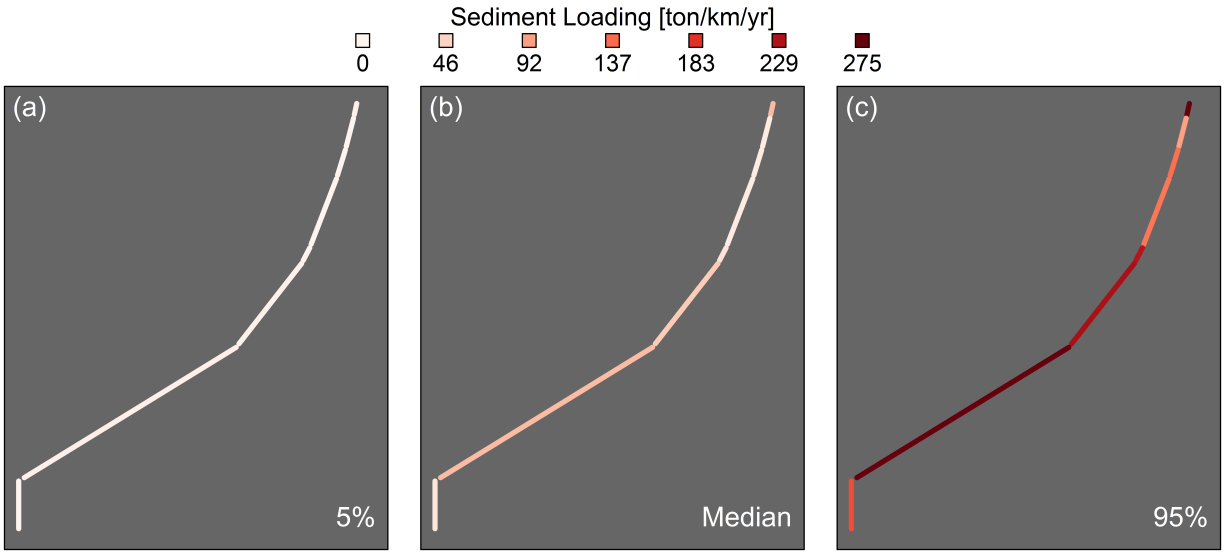

Figure S12: Network schematic of Big Dry Creek showing annual sediment loading rates by modeled reach, normalized by reach length, including the uncertainty range (a and c) and the median of the Monte Carlo results (b). Loading rates are larger than reported in Table 3 in the text because these are cumulative loads over the simulation rather than median annual loads. Results from simulation with $Q_s = 1.0$ transport capacity.

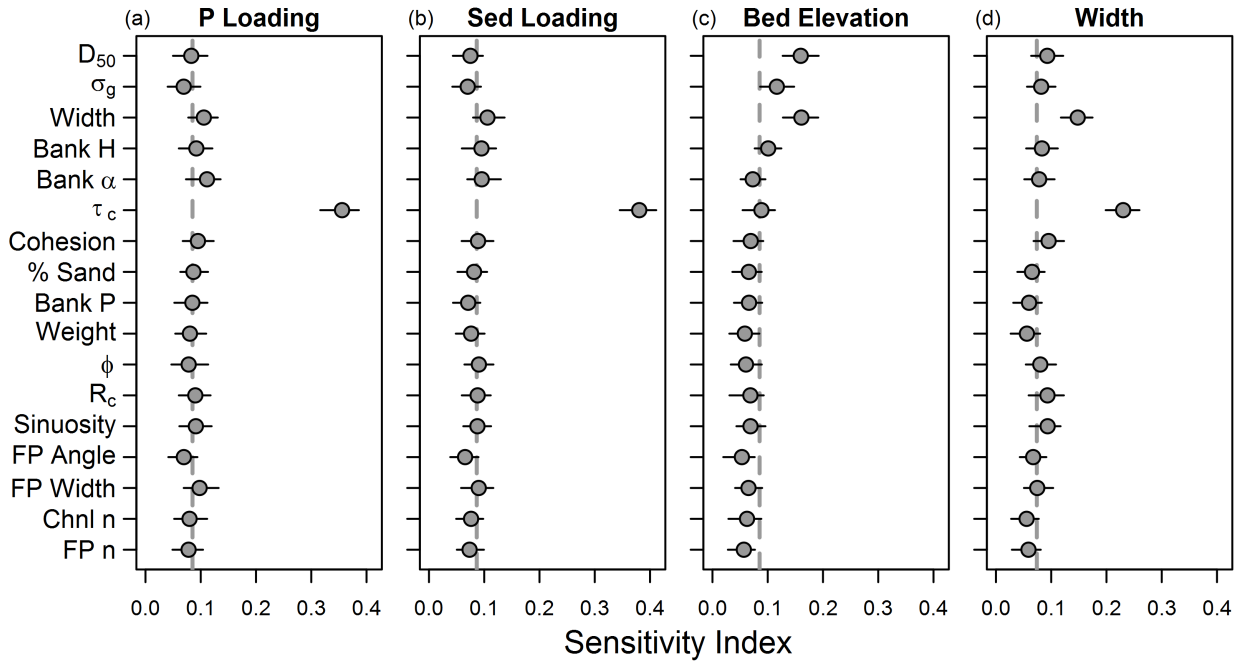

Figure S13: Big Dry Creek sensitivity analysis results for four different model outputs: phosphorus loading (a), sediment loading (b), bed elevation (c), and channel width (d). Points show bias-corrected sensitivity indices with ranges of estimates from bootstrapping. Points below the vertical dashed line had no influence on model output. Results from model runs with $Q_s = 1.0$ transport capacity.

5.3 Lick Creek, Loading Results

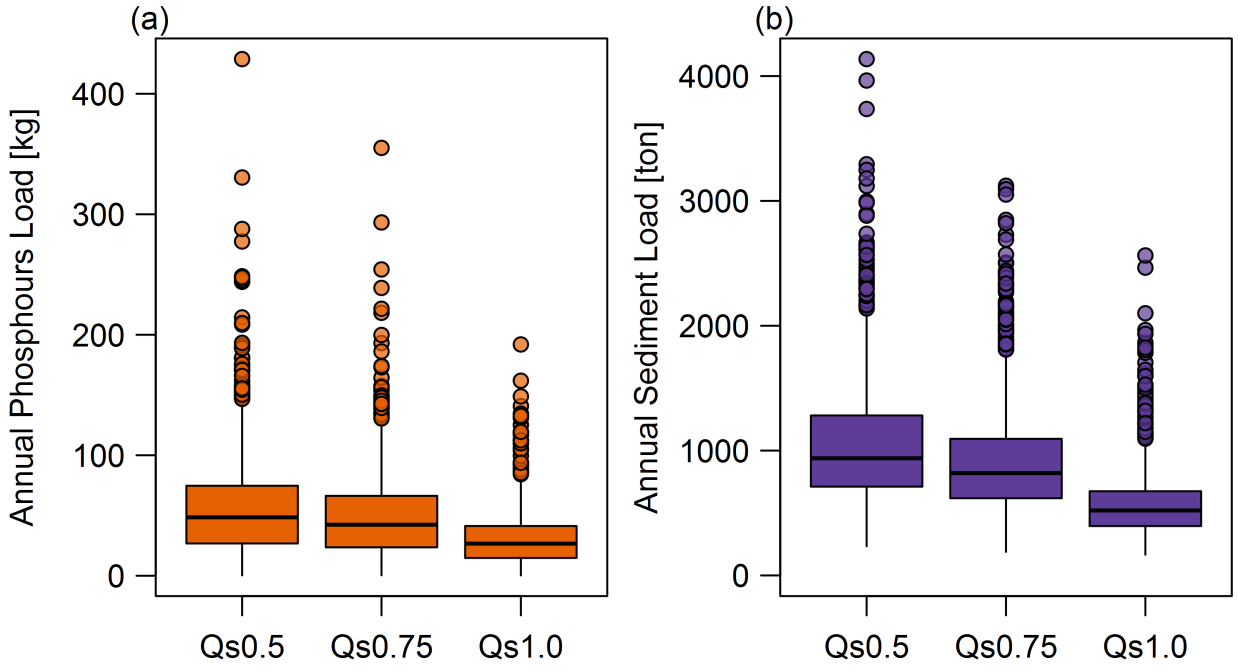

Figure S14: Distributions of median annual phosphorus (a) and sediment (b) loads in Lick Creek across the years of the simulation, for the three different modeled scenarios: $Q_s = 0.5$, $Q_s = 0.75$, and $Q_s = 1.0$ of transport capacity.

5.4 Lick Creek, $Q_s = 0.5$

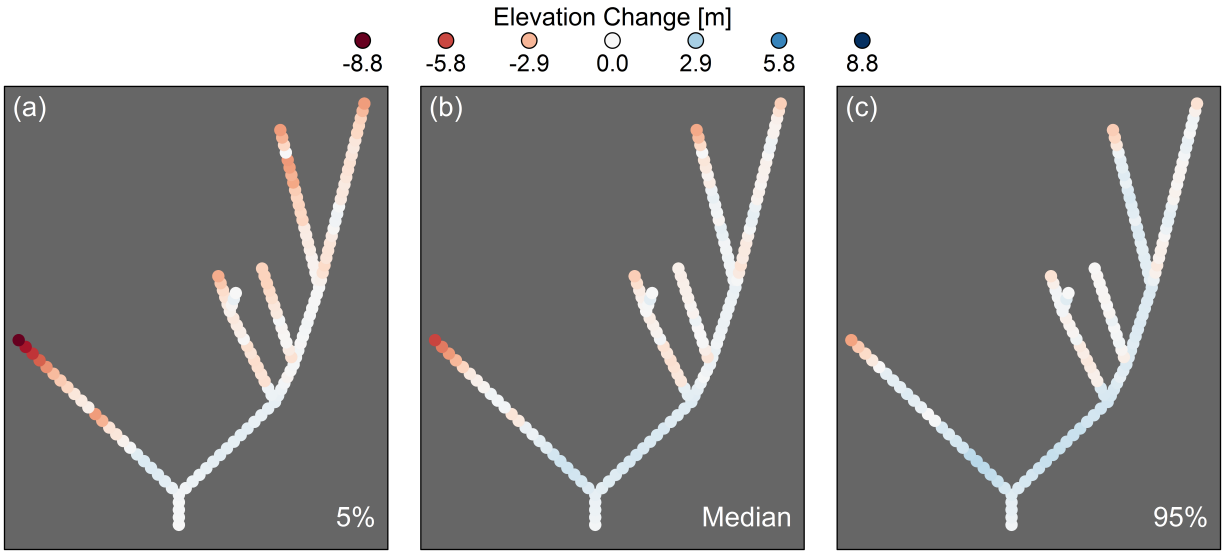

Figure S15: Changes in bed elevation throughout the Lick Creek watershed, including the median results and 5^{th} and 95^{th} percentiles. Model runs from $Q_s = 0.5$ transport capacity.

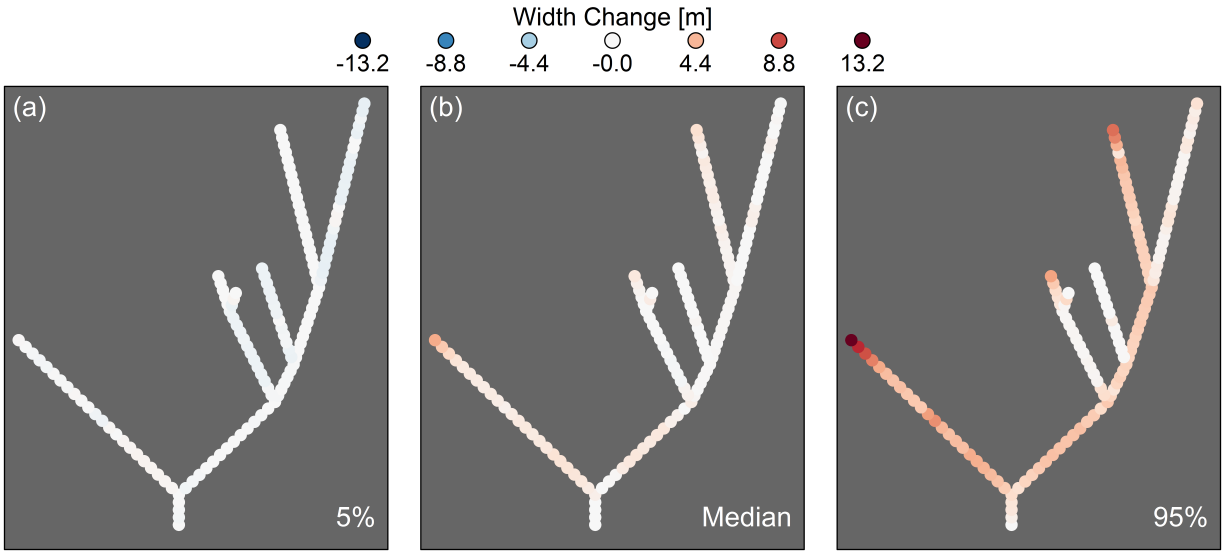

Figure S16: Changes in channel width throughout the Lick Creek watershed, including the median results and 5^{th} and 95^{th} percentiles. Model runs from $Q_s = 0.5$ transport capacity.

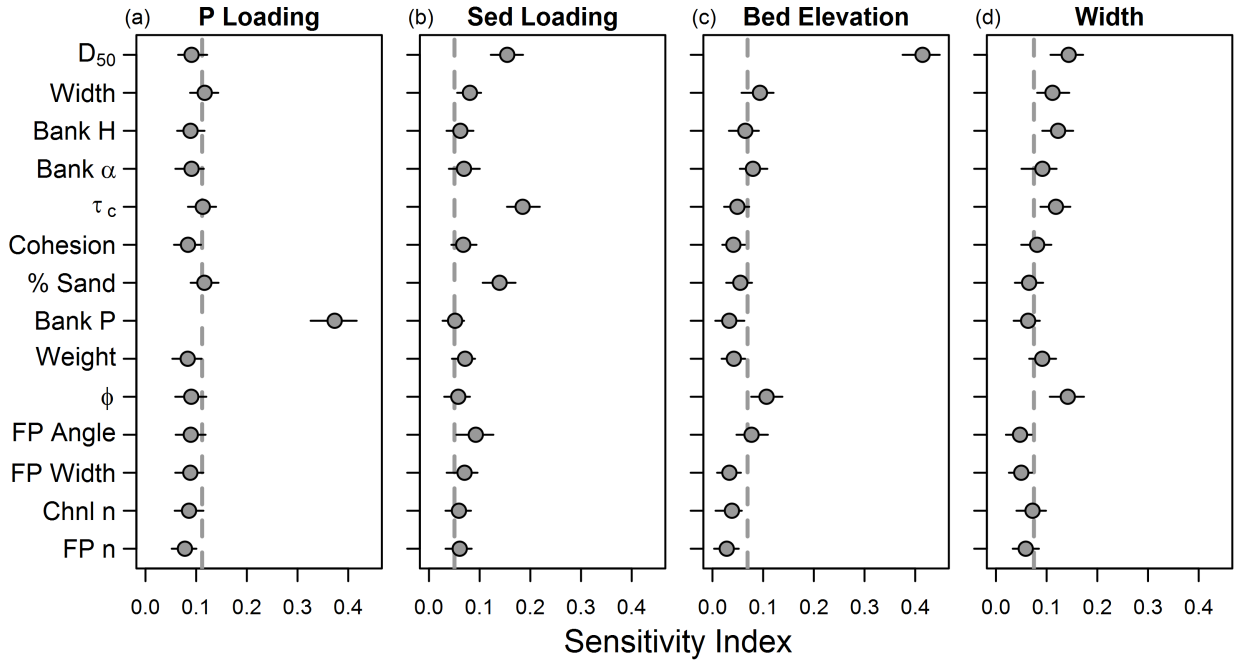

Figure S17: Lick Creek sensitivity analysis results for four different model outputs: phosphorus loading, sediment loading, bed elevation, and channel width. Points show bias-corrected sensitivity indices with ranges of estimates from bootstrapping. Points below the vertical dashed line had no influence on model output. Results from model runs where $Q_s = 0.5$ transport capacity.

5.5 Lick Creek, $Q_s = 0.75$

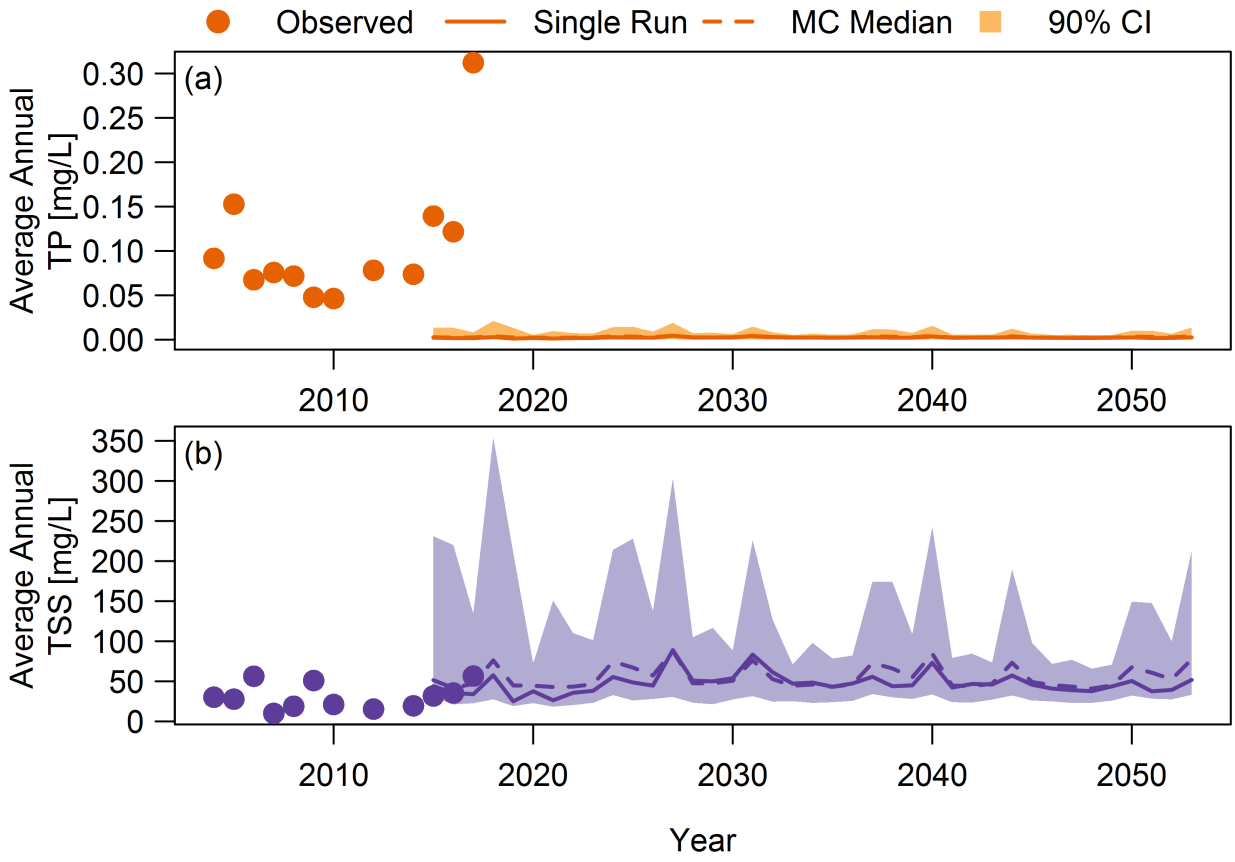

Figure S18: Measured TP and TSS concentrations in Lick Creek at the watershed outlet, along with modeled projections for the single run and median and 90% CI for the Monte Carlo simulations. Model runs from $Q_s = 0.75$ transport capacity.

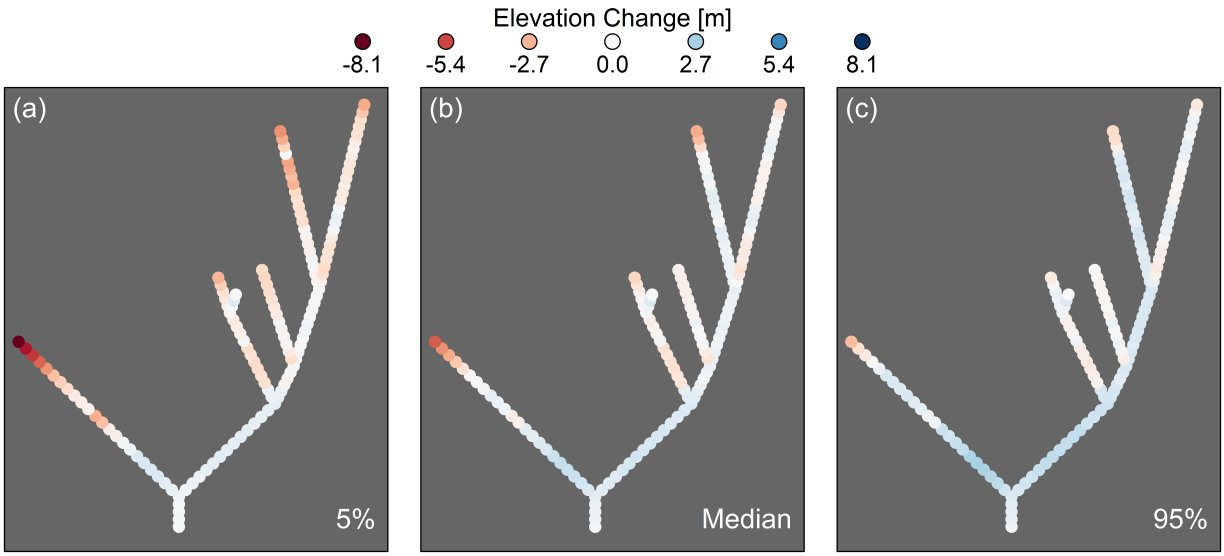

Figure S19: Changes in bed elevation throughout the Lick Creek watershed, including the median results and 5^{th} and 95^{th} percentiles. Model runs from $Q_s = 0.75$ transport capacity.

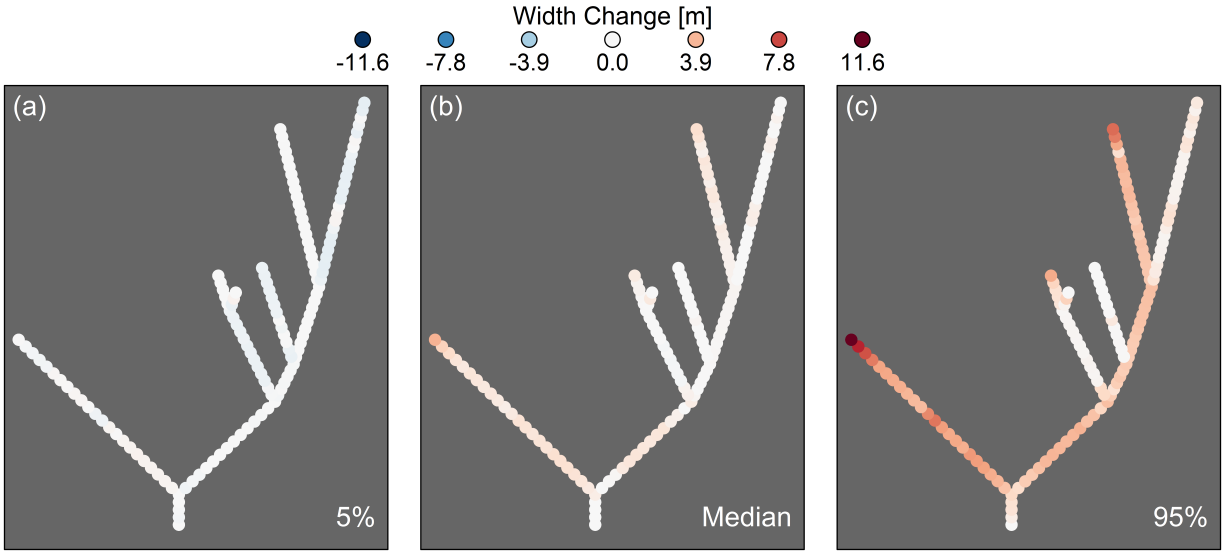

Figure S20: Changes in channel width throughout the Lick Creek watershed, including the median results and 5^{th} and 95^{th} percentiles. Model runs from $Q_s = 0.75$ transport capacity.

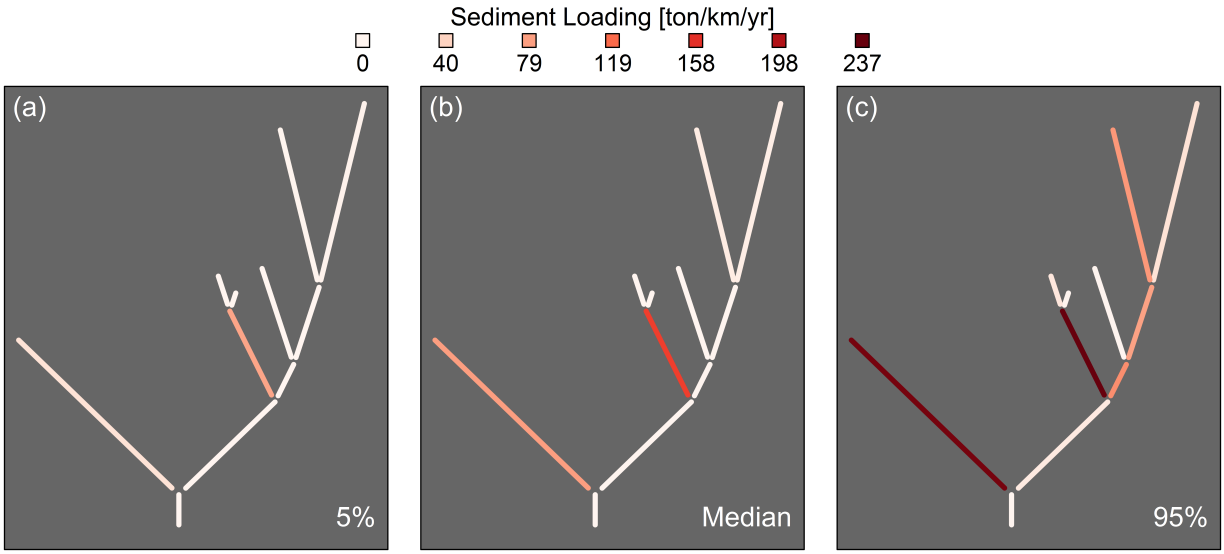

Figure S21: Network schematic of Lick Creek showing annual sediment loading rates by modeled reach, normalized by reach length including the uncertainty range (a and c) and the median of the Monte Carlo results (b). The two reaches with highest loading rates both had actively migrating knickpoints. Loading rates are larger than reported in Table 3 in the text because these are cumulative loads over the simulation rather than median annual loads. Results from simulation with $Q_s = 0.75$ transport capacity.

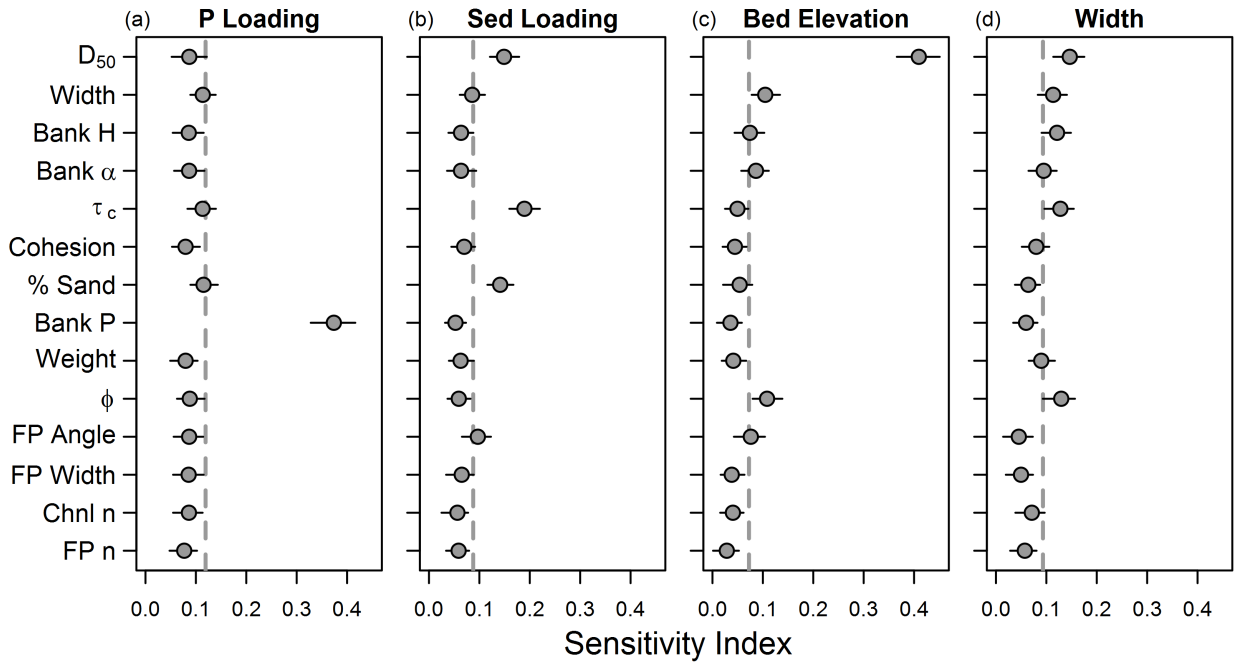

Figure S22: Lick Creek sensitivity analysis results for four different model outputs: phosphorus loading, sediment loading, bed elevation, and channel width. Points show bias-corrected sensitivity indices with ranges of estimates from bootstrapping. Points below the vertical dashed line had no influence on model output. Results from model runs where $Q_s = 0.75$ transport capacity.

5.6 Lick Creek, $Q_s = 1.0$

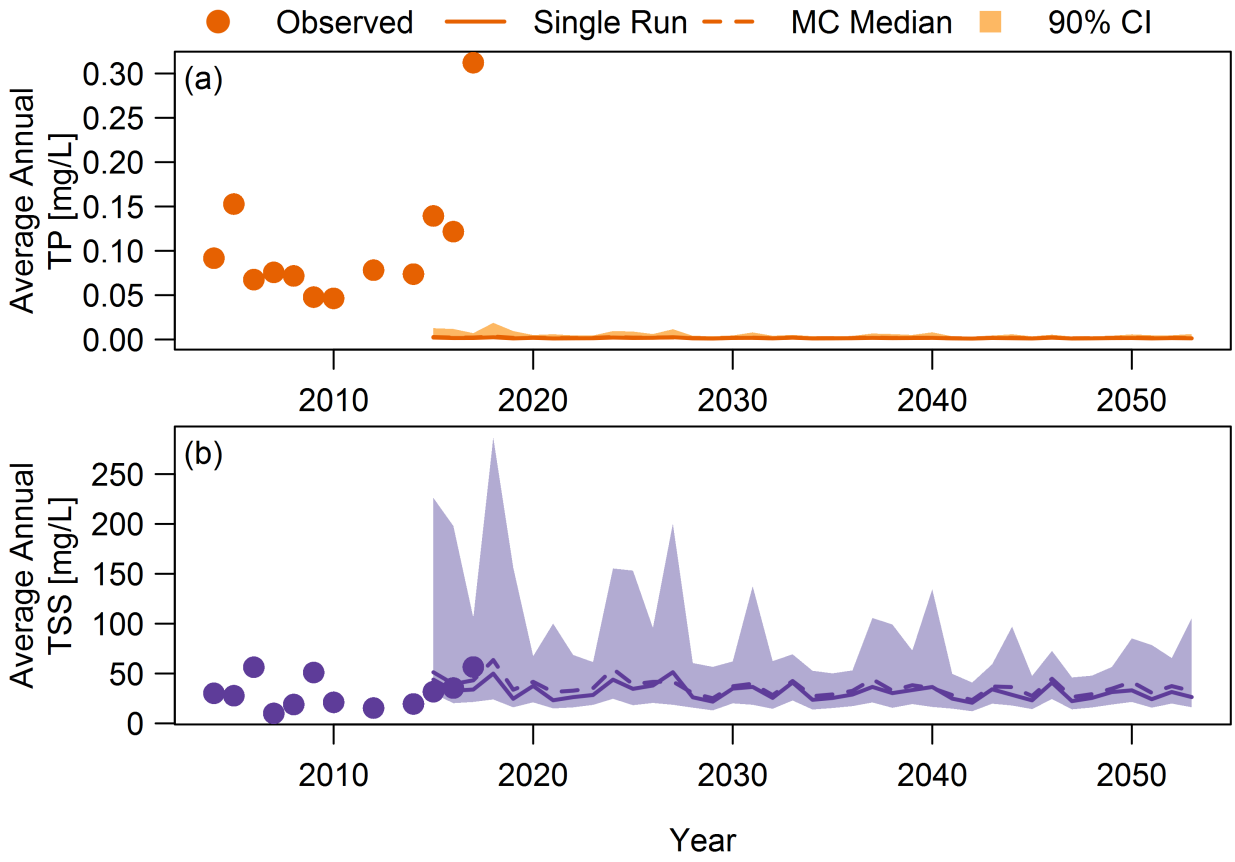

Figure S23: Measured TP and TSS concentrations in Lick Creek at the watershed outlet, along with modeled projections for the single run and median and 90% CI for the Monte Carlo simulations. Model runs from $Q_s = 1.0$ transport capacity.

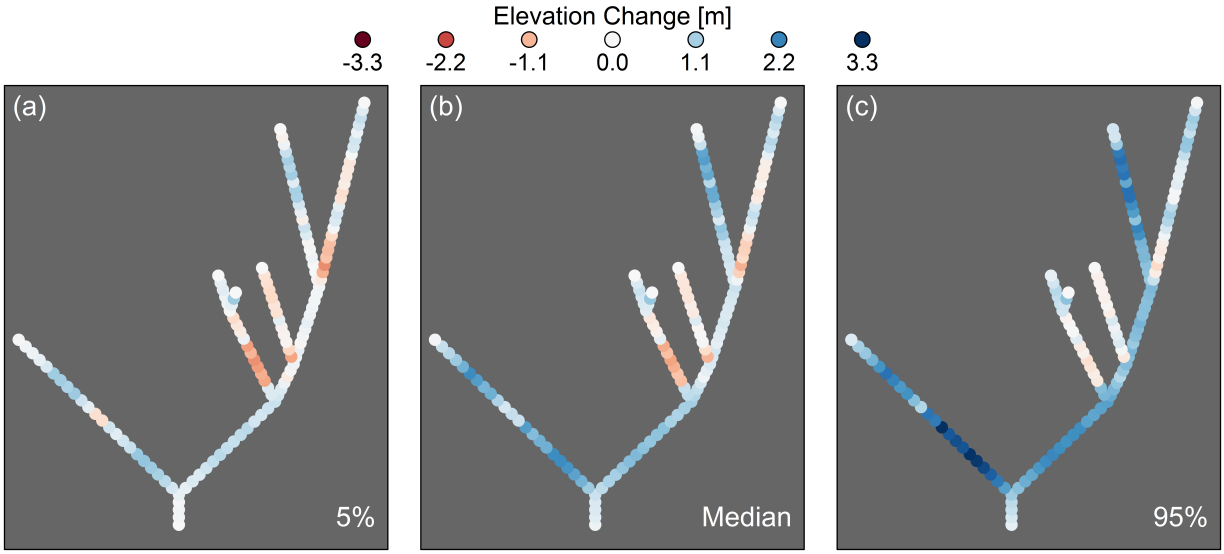

Figure S24: Changes in bed elevation throughout the Lick Creek watershed, including the median results and 5^{th} and 95^{th} percentiles. Model runs from $Q_s = 1.0$ transport capacity.

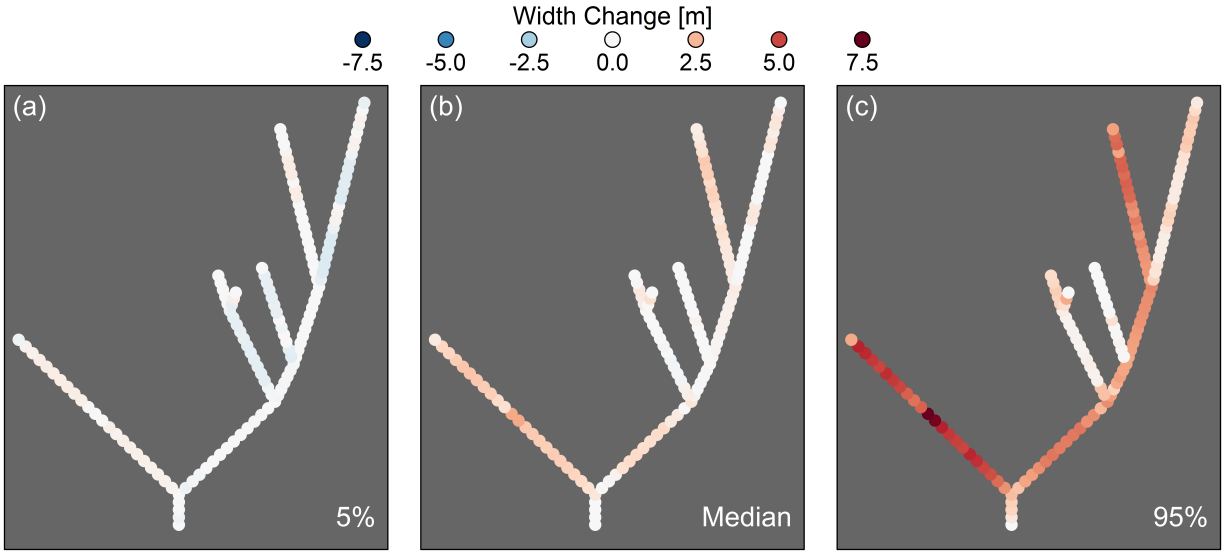

Figure S25: Changes in channel width throughout the Lick Creek watershed, including the median results and 5^{th} and 95^{th} percentiles. Model runs from $Q_s = 1.0$ transport capacity.

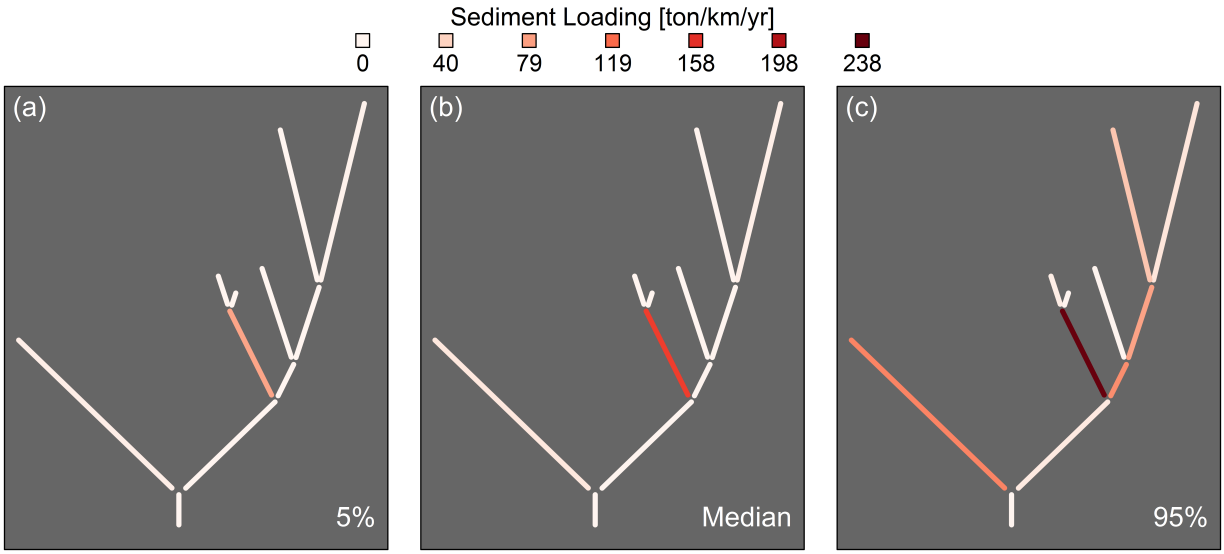

Figure S26: Network schematic of Lick Creek showing annual sediment loading rates by modeled reach, normalized by reach length including the uncertainty range (a and c) and the median of the Monte Carlo results (b). The two reaches with highest loading rates both had actively migrating knickpoints. Loading rates are larger than reported in Table 3 in the text because these are cumulative loads over the simulation rather than median annual loads. Results from simulation with $Q_s = 1.0$ transport capacity.

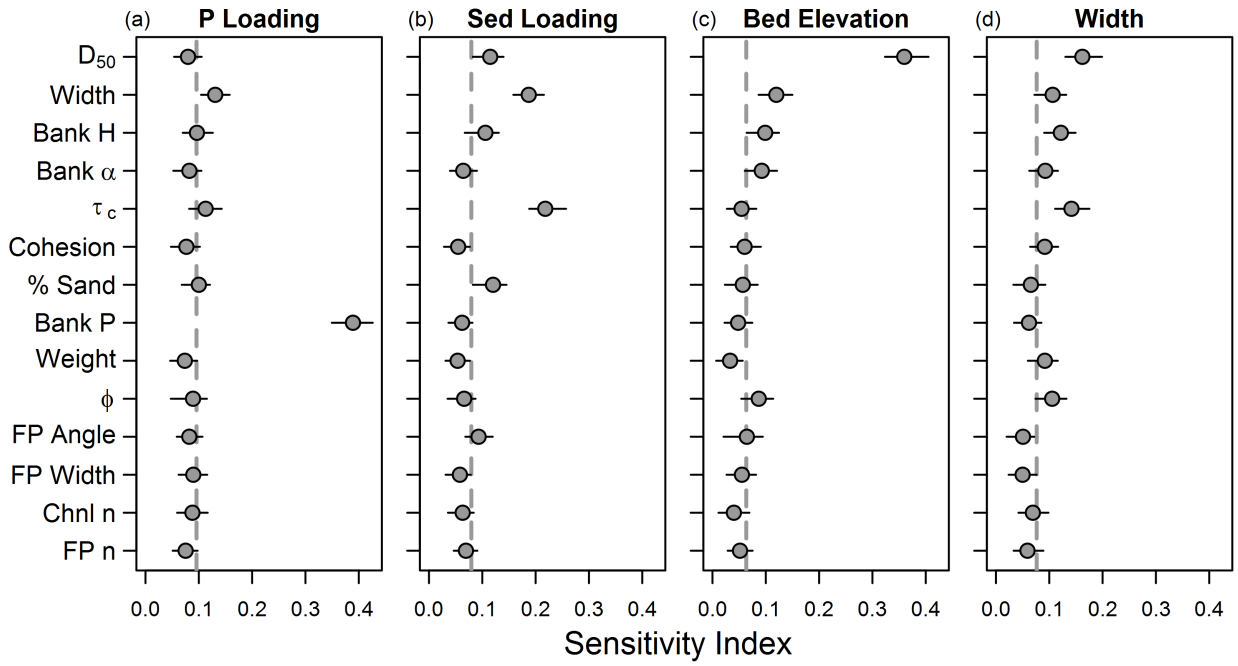

Figure S27: Lick Creek sensitivity analysis results for four different model outputs: phosphorus loading, sediment loading, bed elevation, and channel width. Points show bias-corrected sensitivity indices with ranges of estimates from bootstrapping. Points below the vertical dashed line had no influence on model output. Results from model runs where $Q_s = 1.0$ transport capacity.

References

Army Corps of Engineers (1970), Hydraulic design of flood control channels, *Tech. rep.*, EM 1110-2-1601, Department of the Army.

Jaeger, K. L., E. E. Wohl, and A. Simon (2010), A comparison of average rates of alluvial erosion between the south-western and south-eastern United States, *Earth Surface Processes and Landforms*, *35*(4), 447–459, doi:10.1002/esp.1960.

Manson, S., J. Schroeder, D. Van Riper, and S. Ruggles (2017), IPUMS National Historical Geographic Information System: Version 12.0 [Database], doi:10.18128/D050.V12.0.

Rosburg, T. T., P. A. Nelson, and B. P. Bledsoe (2017), Effects of urbanization on flow duration and stream flashiness: A case study of Puget Sound streams, Western Washington, USA, *Journal of the American Water Resources Association*, *53*(2), 493–507, doi:10.1111/1752-1688.12511.

Simon, A., R. E. Thomas, and L. Klimetz (2010), Comparison and experiences with field techniques to measure critical shear stress and erodibility of cohesive deposits, *2nd Joint Federal Interagency Conference, Las Vegas*, *826*.

Simon, A., N. Pollen-Bankhead, and R. E. Thomas (2011), Development and application of a deterministic bank stability and toe erosion model for stream restoration, in *Stream Restoration in Dynamic Fluvial Systems: Scientific Approaches, Analyses, and Tools*, edited by A. Simon, S. Bennett, and J. Castro, pp. 453–474, American Geophysical Union, Washington, D.C.